# Identification and functional characterization of two heme uptake systems required for virulence of the fish pathogen *Flavobacterium psychrophilum*

Yueying Zhu[1], Delphine Lechardeur[2], Jean-François Bernardet[1], Brigitte Kerouault[1], Cyprien Guérin[3], Dimitri Rigaudeau[4], Pierre Nicolas[3], Eric Duchaud[1] and Tatiana Rochat[1*]

[1] Université Paris-Saclay, INRAE, UVSQ, VIM, Jouy-en-Josas, France
[2] Université Paris-Saclay, INRAE, AgroParisTech, Micalis Institute, Jouy-en-Josas, France
[3] Université Paris-Saclay, INRAE, MaIAGE, Jouy-en-Josas, France
[4] INRAE, UE IERP, Jouy-en-Josas, France.

* Corresponding author
E-mail: tatiana.rochat@inrae.fr

# Abstract

*Flavobacterium psychrophilum*, a member of the phylum *Bacteroidetes,* causes bacterial cold-water disease in salmonids worldwide. Infected fish exhibit tissue damages and develop hemorrhagic septicemia. The molecular factors involved in host colonization are mostly unknown. In this study, we identified two TonB-dependent receptors that are required for iron homeostasis and virulence in rainbow trout (*Oncorhynchus mykiss*). Transcriptional analyses revealed that their expression is tightly controlled and upregulated under specific iron sources and concentrations. Characterization of single and double deletion mutants showed that the two receptors act without redundancy: BfpR is required for optimal growth in the presence of high hemoglobin level, while HfpR confers the capacity to acquire nutrient iron from heme or hemoglobin under iron scarcity. The gene *hfpY*, co-transcribed with *hfpR*, encodes a protein belonging to the HmuY family but with low sequence conservation compared to other members of this family. We demonstrated that HfpY is able to bind heme *in vitro* and contributes significantly to host colonization and disease severity in experimentally infected rainbow trout. Overall, these results are consistent with a model in which both BfpR and Hfp systems promote heme uptake and respond to distinct signals to adapt iron acquisition to the different stages of pathogenesis. Our findings give insight into the molecular basis of *F. psychrophilum* pathogenicity and point to the newly identified heme outer membrane receptors as promising targets for antibacterial development.


# Author summary

Infectious diseases are a major threat for human and animal health. Bacterial pathogens impact aquaculture, a sector that accounts for half of the human fish consumption, and mechanistic insights into pathogenesis allow for improved control strategies. Pathogens have to retrieve

essential nutrients to multiply. Host-derived heme constitutes the largest iron source during infection and pathogens have evolved fine-tuned iron acquisition systems to overcome host scavenging mechanisms while preventing iron toxicity. These mechanisms are poorly understood in pathogens of the family *Flavobacteriaceae* that have a critical impact on the fish farming, animal welfare and environment. Here, we report the identification and characterization of two heme uptake systems important for adaptation under distinct iron sources conditions encountered during infection and for virulence and host colonization in *Flavobacterium psychrophilum*, a serious pathogen of salmonids.

53 # Introduction

54 Aquaculture is a rapidly growing sector which now represents more than half of the human
55 fish consumption in the world [1]. However, its sustainable development faces the major challenge
56 of controlling infectious diseases caused by poorly known aquatic pathogens. These include several
57 Gram-negative bacteria belonging to the family *Flavobacteriaceae* (phylum *Bacteroidetes*), of
58 which a majority of members are commensals and saprophytes commonly isolated from
59 environmental sources such as soil, sediments and water [2]. Among them, *Flavobacterium*
60 *psychrophilum* infects salmonids in freshwater environments and is responsible for diseases known
61 as rainbow trout fry syndrome and bacterial cold-water disease which constitute a major chronic
62 health issue for the fish farming industry worldwide [3-8]. *F. psychrophilum* outbreaks cause
63 complex rearing issues and substantial economic losses, impact animal welfare and -due to repeated
64 use of antibiotics- the environment. A better understanding of the pathogenesis and biology of this
65 pathogen is needed to enhance the development of alternative control strategies, such as efficient
66 vaccines, bacteriophages therapy and selection of resistant fish lines [9-12].

67 Juveniles of rainbow trout (*Oncorhynchus mykiss*) are particularly susceptible. In fry, the
68 disease results in septicaemia leading to mortalities rising up to 70% without appropriate antibiotic
69 treatment. Infected fish present signs of tissue erosion and necrotic lesions, typically in the jaw, the
70 caudal peduncle or the caudal fin [13]. The bacterium is mainly found in the damaged skin and
71 muscular tissues surrounding the lesions, in the lymphoid organs, particularly in the spleen that
72 exhibits hemorrhages and hypertrophy, and harbours a large number of bacteria [14-16]. *F.*
73 *psychrophilum* cells are highly proteolytic, cytotoxic and possess adhesion abilities [17-20]. The
74 Type IX secretion system (T9SS) is required for pathogenicity and several secreted adhesins,

75 peptidases and other uncharacterized proteins likely play a role in adhesion to host cells, tissue
76 degradation and pathogen spreading [21-23].

77 Within the host, *F. psychrophilum* cells face a strong inflammatory response [24, 25]. Host
78 colonization relies on the resistance to stresses and the ability to efficiently retrieve nutrients such
79 as amino acids, vitamins and essential metals. In vertebrates, iron is mainly sequestered in iron- or
80 heme-binding proteins preventing toxic effects of free iron and limiting accessibility for bacterial
81 growth. Pathogens have developed sophisticated mechanisms to fulfil their iron needs from various
82 sources [26]. In Gram-negative bacteria, many of the iron acquisition systems rely on TonB-
83 dependent receptors (TBDR) which mediate the active uptake of specific substrates across the outer
84 membrane. TBDRs are β-barrels outer membrane proteins forming pores that are occluded by a
85 globular periplasmic domain (plug) in the absence of substrate. Substrate transport is energized by
86 the inner membrane TonB-ExbBD complex that transduces energy derived from the proton motive
87 force [27]. A large variety of iron uptake TBDRs have been described, involving either the direct
88 binding of host iron- or heme-binding proteins by the receptor, or the indirect substrate capture by
89 high-affinity siderophores or hemophores. Expression of these genes are typically tightly regulated
90 in response to iron availability in order to meet bacterial needs for iron while avoiding toxicity of
91 excessive intracellular iron concentrations [28].

92 Despite the importance of iron homeostasis, the genes involved in iron uptake remain
93 uncharacterized in *F. psychrophilum*. *In vitro*, growth of the bacterium is strongly inhibited by
94 addition of an iron chelator, but can be restored by the supply of hemoglobin or transferrin,
95 suggesting that the bacterium is able to uptake iron from these compounds [29]. Production of
96 siderophores, hemolysis activity and hemoglobin consumption have been reported [18, 21, 29]. In
97 addition, the inactivation of *exbD2*, a subunit of the TonB system, results in impaired growth under

98 iron restricted conditions [30], pointing out the probable existence of TonB-dependent iron uptake
99 systems in *F. psychrophilum*.

100 Here, we took advantage of a large *in vitro* condition-dependent transcriptome dataset [31]
101 to identify iron-regulated TBDR encoding genes. By combining reverse genetics, *in vitro*
102 phenotyping of deletion mutants and experimental infection in rainbow trout, we demonstrate the
103 importance of two heme/hemoglobin receptors for the virulence of *F. psychrophilum*. The first
104 receptor, that we named BfpR, acts under high-level hemoglobin conditions. The second receptor,
105 HfpR, acts under iron-restricted conditions in concert with its cognate hemophore HfpY, a new
106 member of the HmuY family widespread in the phylum *Bacteroidetes*.

107 # Results

108 ## Identification of two TonB-dependent receptors with potential
109 function in heme utilization

110 The distribution of TBDRs was analyzed in a collection of 22 genomes of *F. psychrophilum*
111 isolates representative of a variety of host species, geographical origins and clonal complexes [32].
112 A total of 33 TBDR-encoding genes were retrieved. With an average number of 25 per genome,
113 most (21) of these predicted TBDRs were conserved in all isolates, though 3 were pseudogenes in
114 one isolate (Fig 1). Only a few TBDRs have predicted substrates, among which are the cobalamin
115 transporter BtuB and 2 putative receptors homologous to the ferric hydroxamate receptor FhuA
116 and the ferric citrate transporter FecA [33]. Among TBDR genes found only in a subset of the
117 isolates, 3 may be associated to a particular host fish species. The first one, THC0290_1129 in
118 strain OSU THCO2-90, is only present in the genomes of CC-ST9 isolates infecting coho salmon.
119 The 2 others, FP2456 and FP1882 in strain JIP 02/86, are present in all isolates belonging to the
120 clonal complexes associated with rainbow trout (CC-ST10 and CC-ST90), but truncated and absent
121 in the other genomes, respectively.

122 In order to further identify, among these TBDRs, those that are involved in iron acquisition,
123 we searched for genes whose expression profile indicated specific regulation under blood
124 supplementation, fish plasma exposure or conditions of iron limitation in the condition-dependent
125 transcriptome dataset previously established for strain OSU THCO2-90 [31]. Two TBDR genes
126 were up-regulated in the presence of blood: (i) THC0290_0369 without predicted substrates, and
127 (ii) THC0290_1679, a member of the heme/hemoglobin receptor family (TIGR01785), hereafter
128 named *bfpR* (for blood-induced *Flavobacterium psychrophilum* receptor). *bfpR* was also

129 overexpressed in the presence of fish plasma but was not modulated by iron limitation. Four TBDR-
130 encoding genes were up-regulated in cells submitted to low-iron conditions, but down-regulated
131 when blood was supplied (Fig 1 and F1 in *Supporting Information*): (i-ii) FhuA and FecA
132 siderophore receptors homologs; (iii) THC0290_0681 with unknown substrate; and (iv)
133 THC0290_1814, the most highly deregulated gene, hereafter named *hfpR* (for heme *F.*
134 *psychrophilum* receptor). *hfpR* is conserved in synteny with a gene encoding a HmuY-like
135 hemophore protein (hereafter named *hfpY*), suggesting functional similarity with the heme
136 utilization system Hmu characterized in other *Bacteroidetes* [34-37].

137 Here, we further characterized the BfpR and Hfp systems predicted to transport heme.
138 Expression profiles suggesting a distinct regulation of the corresponding genes (F1 in *Supporting*
139 *Information*), we thus examined their transcriptional structure and regulation (see below). To
140 analyze their respective role in bacterial growth, we also constructed the single and double deletion
141 mutants Δ*bfpR*, Δ*hfpR*, Δ*hfpY* and Δ*hfpR*Δ*bfpR*, by allelic replacement in *F. psychrophilum* OSU
142 THCO2-90 (T1 in *Supporting Information*). The ectopic complementation of these mutants was
143 performed by inserting a single gene copy under the control of the native promoter at a different
144 chromosomal position than the endogenous deleted gene copy. For Δ*hfpR*Δ*bfpR*, the 2 genes were
145 inserted arranged in tandem. For this purpose, a new plasmid was designed allowing chromosomal
146 gene insertion at a neutral site conserved within the *F. psychrophilum* species and the efficacy of
147 this expression platform was validated using reporter genes (F2 and F3 in *Supporting Information*).
148 The growth of the mutants was analyzed *in vitro* under different conditions of iron and *in vivo* in
149 the natural host.
150

151 **High levels of hemoglobin promote the accumulation of monocistronic**

152 ***bfpR* mRNA**

153 BfpR is encoded downstream of the aspartate-semialdehyde dehydrogenase (*asd*) and a
154 hypothetical protein (THC0290_1678; Fig 2A). Structure of the *bfpR* transcript is uncertain:
155 expression level across biological conditions differs between *bfpR, asd* and THC0290_1678, and
156 the increase of mRNA level in colonies grown on blood-supplemented TYES agar occurs upstream
157 *bfpR*, suggesting that *bfpR* is transcribed as a monocistronic mRNA. However, no transcription
158 start site (TSS) was detected in the corresponding region (Fig 2A)[31].

159 Several methods were combined to define the structure of the *bfpR* transcript. First, a
160 putative polycistronic mRNA encompassing *asd*, THC0290_1678 and *bfpR* was predicted by RT-
161 PCR using overlapping primers. Circular 3'-5' RACE experiments were then run in an attempt to
162 identify the most abundant *bfpR* transcript and to distinguish between primary and processed RNAs
163 (Fig 2A; F4 in *Supporting Information*). *bfpR* amplification from a primer within *asd* was
164 unsuccessful, attesting of the very low quantity of the polycistronic mRNA predicted by
165 overlapping RT-PCR. In contrast, cDNA was successfully amplified using primers within *bfpR*.
166 The majority of transcripts ended at +83 bp relative to the *bfpR* stop codon, while no discrete 5'-
167 end position was identified. Instead, most transcripts started within a ~50 bp-long region spanning
168 from -399 to -347 bp relative to the *bfpR* start codon, which coincides with the upshift of expression
169 signal detected by microarrays in blood supply conditions. By using a primer within
170 THC0290_1678, transcripts were detected by nested PCR only and started mainly at -673 (±1) bp
171 relative to *bfpR* start codon. This 5' end is 22 bp downstream the start position of THC0290_1678.
172 However, the location of translation initiation is difficult to predict in *Bacteroidetes* [38] and
173 another ATG codon located 38 bp downstream the 5' end may be the correct start. Various

174 fragments (306, 609 and 950 bp) of the upstream region of *bfpR* were cloned into a transcriptional
175 reporter plasmid and a significant promoter activity was detected only for the one carrying the
176 longest fragment when colonies were grown in TYES agar supplemented with 1% hemoglobin (Fig
177 2B). These results indicate that the majority of *bfpR* mRNAs are monocistronic and may originate
178 from processing of a longer transcript starting 673 bp upstream of *bfpR*.

179 We therefore compared the effect of hemoglobin supply on *bfpR* mRNA level by RT-qPCR
180 assays (Fig 2C). Addition of large amounts of hemoglobin in TYES broth led to 10-fold increase
181 of *bfpR* mRNA level. This increase was not observed for the upstream gene THC0290_1678.
182 Altogether, we concluded that a primary transcript encompassing THC0290_1678 and *bfpR* is
183 synthetized then probably subject to maturation, resulting in the *bfpR* mRNA that accumulates in
184 presence of large amounts of hemoglobin.

185

## 186 BfpR contributes to growth in the presence of high amounts of 187 hemoglobin

188 On the basis of its expression profile, we analyzed the role of BfpR on the growth of *F.*
189 *psychrophilum* under high-hemoglobin condition. The wild-type strain exhibited a slight delay in
190 the presence of 1% hemoglobin (equivalent of 620 µM heme), but final viable cell counts were
191 higher than in TYES broth (F5 in *Supporting Information*), indicating that hemoglobin availability
192 can enhance bacterial growth. In these conditions, the growth rate of Δ*bfpR* was reduced compared
193 to that of the wild-type and partially restored in the complemented Δ*bfpR* strain (Fig 3). RT-qPCR
194 showed that ectopic expression of *bfpR* in this complemented Δ*bfpR* strain resulted in reduced
195 mRNA level compared to the wild-type (F6 in *Supporting Information*), indicating that adequate
196 regulation of *bfpR* expression is important for growth in these conditions. Growth curves of

197 Δ*hfpR*Δ*bfpR* and Δ*bfpR* were similar. These results showed that among the two TBDRs, only BfpR
198 is required for optimal growth in the presence of high amounts of hemoglobin.
199

## 200 The *hfp* operon is transcribed in response to iron scarcity

201 The Hmu systems characterized so far in *Porphyromonas gingivalis* and other
202 *Bacteroidetes* are transcribed in a polycistronic transcript encoding at least 1 HmuY-like
203 hemophore, 1 TBDR and 4 uncharacterized proteins (a putative CobN/magnesium chelatase and 3
204 putative membrane proteins) [36, 37]. In *F. psychrophilum*, only the genes encoding a TBDR (*hfpR*)
205 and the HmuY-like protein (*hfpY*) are present. They are located within a 19 kb region containing
206 other iron-responsive transcripts encoding proteins that have a putative role in iron assimilation or
207 transmembrane electron transfer (T2 in *Supporting Information*)[31, 39]. The upregulated
208 polycistronic mRNA deduced from transcriptomic data is bound by a putative TSS and a predicted
209 intrinsic terminator and encodes, from 5' to 3': (i) HfpR; (ii) THC0290_1813, a predicted 18 kDa
210 inner membrane protein of unknown function belonging to the DoxX family (IPR032808); and (iii)
211 HfpY (Fig 4A). Expression signal measured by high-density microarrays was higher in the *hfpY*
212 part of the operon for all biological conditions suggesting that a monocistronic *hfpY* mRNA may
213 also be produced (F7 in *Supporting Information*). We confirmed this transcriptional structure by
214 3'-5' RACE experiments: two 5'-ends and one unique 3'-end were identified (Fig 4A; F4B in
215 *Supporting Information*). RppH enzymatic treatment increased cDNA amplification for the
216 polycistronic form only indicating a 5'-triphosphorylated RNA. These results confirmed the TSS
217 position and the existence of 2 mRNAs, while suggesting that the *hfpY* mRNA originates from a
218 post-transcriptional maturation event.

219 Expression of the *hfp* locus was then monitored under iron-depleted and -replete conditions
220 using a transcriptional reporter ($P_{hfpR}$-mCh) and RT-qPCR assays. Addition of the iron-chelator
221 ethylenediamine-*N*,*N'*-bis (2-hydroxyphenylacetic acid) (EDDHA) in TYES broth resulted in a
222 strong increase of promoter activity, which was countered by $FeCl_3$ supply in a dose-dependent
223 manner (Fig 4B). Promoter activity was also limited by heme or hemoglobin supply, although with
224 a lower efficiency than when $FeCl_3$ was used (Fig 4B). RT-qPCR confirmed up-regulation of the
225 3 genes composing the *hfp* operon under iron limitation and the effect of hemoglobin supply (Fig
226 4C). Moreover, a 5-fold down-regulation was measured in the presence of high level of hemoglobin
227 in iron-replete TYES broth (Fig 4C), which is consistent with the down-regulation previously
228 observed by microarrays in the presence of blood [31].
229 We concluded from these results that 2 mRNAs are produced at the *hfp* locus: a primary
230 transcript encompassing *hfpR*, THC0290_1813 and *hfpY,* and a matured mRNA carrying *hfpY* only,
231 resulting in more abundant mRNA for *hfpY* than for *hfpR*. The expression level of these 2 RNAs is
232 tightly controlled in response to iron availability through the regulation of the *hfpR* promoter which
233 is activated by iron scarcity and downregulated in presence of iron sources.
234

## 235 HfpR and HfpY are required for heme utilization under iron scarcity

236 The effect of iron limitation on growth was first analyzed on the wild-type strain. Addition
237 of EDDHA, a chelator of ferric iron Fe(III), to TYES broth resulted in a strong growth inhibition,
238 confirming that iron is an essential element for *F. psychrophilum*. Growth was restored by the
239 supply of hemoglobin, hemin or $FeCl_3$, indicating that the bacterium is able to scavenge these
240 different iron sources from the environment (Fig 5).

241 We then analyzed the role of HfpR and HfpY by comparing the growth of deletion mutants
242 and respective complemented strains under iron scarcity (Fig 5). Supplementation by $FeCl_3$ fully
243 restored the growth of all strains (Fig 5). In contrast, growth inhibition was only partially restored
244 by hemoglobin and hemin supplementation in mutant Δ*hfpR* which still exhibited a severe growth
245 delay compared to complemented Δ*hfpR* and wild-type strains. Δ*hfpY* was by far less affected but
246 its growth rate still significantly reduced compared to the wild-type in hemoglobin supplemented
247 medium containing EDDHA, and this growth defect was partially restored in the complemented
248 Δ*hfpY* strain. In contrast, no growth defect was observed in Δ*hfpY* when hemin was supplied instead
249 of hemoglobin (Fig 5). Partial growth restoration in the ectopic complemented Δ*hfpY* strain is likely
250 due to its reduced *hfpY* mRNA level compared to the wild-type as measured by RT-qPCR (F6 in
251 *Supporting Information*). We also evaluated the growth on hemoglobin of a transposition mutant
252 inactivated in the unknown function gene lying between *hfpR* and *hfpY* (THC0290_1813); no
253 difference was observed compared to the wild-type, indicating that this gene is dispensable for
254 heme utilization under iron-restricted conditions (F8 in *Supporting Information*). Finally, the
255 behavior of Δ*bfpR* was analyzed. In contrast to Δ*hfpR* and Δ*hfpY*, no growth defect was observed
256 under iron limitation when hemoglobin, hemin or $FeCl_3$ was supplied, and growth of Δ*hfpR*Δ*bfpR*
257 was indistinguishable from that of Δ*hfpR* (Fig 5). We concluded that HfpR and HfpY are important
258 for utilization of heme compounds under iron scarcity while BfpR is dispensable, and that there is
259 no functional compensation by other genes for the lack of HfpR under these conditions.
260

## 261 *F. psychrophilum* HfpY is a heme-binding protein

262 HfpY exhibits only low level of similarity with other HmuY-like hemophores (below 26%
263 identity in amino-acids sequence; F9 in *Supporting Information*); we thus investigated the ability

264 of HfpY to bind heme *in vitro*. Recombinant HfpY was purified as a fusion to the maltose-binding
265 protein (MBP) from *E. coli*. Spectroscopic monitoring showed that while the maximum absorbance
266 of free hemin was located between 361 and 384 nm, addition of purified MBP-HfpY resulted in a
267 Soret peak at $\lambda_{max}$ 398 nm typical of heme coordination to protein (Fig 6A). Q bands were also
268 visible at 503, 530 and 623 nm in the difference spectra. Heme titration assays indicated a
269 stoichiometry of 1:1 for the holoprotein which is similar to the other characterized HmuY-like
270 hemophores (Fig 6B). Based on these results, we concluded that HfpY of *F. psychrophilum* is a
271 heme-binding protein.
272

## 273 The two TBDRs are required for virulence in rainbow trout

274 Wild-type, deletion mutants and complemented strains were analyzed for virulence in
275 rainbow trout using three experimental infection models that differ by the infection route and fish
276 size. The roles of *hfpR, hfpY* and *bfpR* were first evaluated by measuring bacterial loads in organs
277 after immersion challenge in fry (2 g), a model that mimics the natural route of infection. At 6 h
278 post-infection, *F. psychrophilum* was detected in the gill of fish from all infected groups at a similar
279 concentration (average of 9 x $10^3$ CFU/gill). In contrast, colonization of spleen was significantly
280 lower for groups infected with Δ*hfpR,* Δ*hfpY* or Δ*hfpR*Δ*bfpR* relative to the wild-type (Fig 7A). No
281 significant difference was observed between bacterial loads of fish infected with Δ*bfpR* or the wild-
282 type, though values were more scattered with Δ*bfpR*. Bacterial colonization of the spleen was fully
283 restored by complementation of the Δ*hfpR*Δ*bfpR* double mutant compared to the wild-type, but
284 only partially restored in the complemented Δ*hfpY* strain.

285 Survival curves were then compared in fry (mean weight, 5 g) after intramuscular injection
286 to quantity the virulence. At an infection dose corresponding to 10 LD50 of the wild-type strain,

287 100% of fish died rapidly in groups infected with the wild-type or complemented strains whereas
288 mortality was delayed and survival was significantly increased for fish infected with either Δ*hfpR*
289 or Δ*hfpY* (Fig 7B). A similar difference between strains was also observed using a lower infectious
290 dose (F10 in *Supporting Information*). Using this infection model, the survival curves of fish
291 inoculated with Δ*bfpR* or the wild-type were similar. In addition, the levels of mortality observed
292 with Δ*hfpR*Δ*bfpR* and Δ*hfpR* were similar (F10 in *Supporting Information*).

293 Since massive hemolysis may not be encountered in the fry infection model, we also
294 investigated the role of BfpR in virulence on larger fish. Two groups of juvenile rainbow trout
295 (mean weight, 65 g) were infected by intramuscular injection and the survival curves or bacterial
296 loads in blood, spleen and kidney 4-days post-infection were determined. In this model, bacteremia
297 and bacterial loads in spleen and kidney were consistently significantly lower in the group infected
298 with Δ*bfpR* relative to the wild-type (Fig 7C). The fish groups infected with Δ*bfpR* displayed a
299 higher survival rate compared to those infected with the wild-type strain (Fig 7D).

300 Altogether, the results showed that both Hfp and BfpR systems are necessary for full
301 virulence of *F. psychrophilum* in rainbow trout with no apparent functional redundancy.

302

303 # Discussion

304 Here, we report the identification of two heme/hemoglobin outer membrane receptors
305 conserved in the species and demonstrate that they act differently to support bacterial growth, under
306 high hemoglobin condition for BfpR and under iron scarcity for HfpR. We also show by
307 experimental infection in a natural host, the rainbow trout, that both receptors are required for full
308 virulence (Fig 8). The findings have relevance to other important fish pathogens such as
309 *Flavobacterium columnare* and *Tenacibaculum maritimum* that possess homologs of the two
310 uptake systems reported here.

311

312 ## Expression of the *hfp* and *bfpR* loci is tightly regulated and indicates
313 ## a role under distinct iron conditions

314 Complex regulatory mechanisms act in bacterial pathogens to maintain iron at intracellular
315 levels needed for bacterial development and below its toxicity threshold [26, 40]. Here, we show
316 that *hfpR* and *hfpY* are up-regulated in an iron-dependent manner. The promoter of the operon was
317 induced under low-iron condition, whereas availability of ferric iron led to a dose-dependent
318 transcriptional repression, which was also observed in presence of a high level of hemoglobin. In
319 many bacteria, such regulation is mediated by Fur family iron-responsive regulators. Typically,
320 under iron-replete condition the $Fe^{2+}$-Fur holoprotein binds to the promoter of iron-regulated genes
321 thus preventing transcription, while under low-iron apo-Fur is released and transcription occurs
322 [41]. *F. psychrophilum* genome contains one member of the Fur family (THC0290_0812). Several
323 attempts to construct a deletion mutant failed at the second recombination event, plasmid excision

324 resulting only in wild-type genotype. This may be either due to the requirement of the Fur homolog
325 for growth or to impaired expression of the downstream purine biosynthesis gene *purA* [31].
326 Several evidences indicate that post-transcriptional regulatory events occur in both *bfpR*
327 and *hfp* mRNAs. In the wild-type strain, mRNA levels for *hfpY* were higher than for *hfpR* under
328 all tested biological conditions (F7 in *Supporting Information*)[31]. In-depth analysis of the
329 transcriptional structure of the *hfp* locus revealed the existence of two mRNAs (*hfpR-1813-hfpY*
330 and *hfpY*) and only the polycistronic RNA was triphosphorylated at the 5' terminus, indicating a
331 single primary transcript. Moreover, no binding site of sigma factor was found in the sequence
332 surrounding the 5' end position of *hfpY* mRNA, which is consistent with a post-transcriptional
333 regulation. We also showed that *hfpY* mRNA level was lower in the Δ*hfpY* strain carrying the
334 chromosomal transcriptional fusion $P_{hfpR}$-*hfpY* than in the wild-type, suggesting that the natural 32-
335 nt 5' untranslated region of *hfpY* mRNA is important for its stability. This lower expression was
336 associated to only partial restoration of *in vitro* and *in vivo* phenotypic defects of Δ*hfpY*, indicating
337 that accurate *hfpY* mRNA quantity is needed for full activity of the Hfp system. Moreover, a
338 putative low permissive transcriptional state of the ectopic chromosomal site is unlikely as *hfpR*
339 mRNA level in complemented Δ*hfpR* carrying the $P_{hfpR}$-*hfpR* fusion was similar than in wild-type.
340 It is noteworthy that several *hmuY* transcripts are also produced in *P. gingivalis,* the monocistronic
341 form being more abundant than the bicistronic *hmuY-hmuR* one, suggesting a similar hemophore
342 upregulation in the two species despite distinct operonic structure [36]. In bacteria, the stability of
343 RNAs released by processing of a polycistronic RNA may differ, which affects the relative
344 expression levels of genes within a same operon. Our hypothesis is that a stable *hfpY* transcript is
345 released after maturation of *hfpR-1813-hfpY* mRNA, resulting in higher quantity of *hfpY* compared
346 to *hfpR*, independently of iron level. A similar regulation was recently described in *Pseudomonas*

347 *aeruginosa* for the *hasR-hasA* operon encoding the hemophore-dependent Has system [42].
348 Production of large amounts of hemophore likely provides a significant advantage to maintain
349 effective concentration relative to its cognate receptor while diffusing into the surrounding
350 environment.

351 In contrast to *hfp*, we showed that *bfpR* mRNA accumulated in the presence of hemoglobin
352 under iron-replete condition. The upregulated RNA was monocistronic and likely originated from
353 maturation of a longer RNA starting at -673 bp from the *bfpR* start codon and carrying a putative
354 hypothetical gene (THC0290_1678). RNA level of the 5' region of this long transcript was
355 unchanged in the presence of hemoglobin. The underlying mechanism, presently not known, likely
356 involves the condition-dependent modulation of *1678-bfpR* mRNA cleavage by a ribonuclease.
357 Typically, such regulation can be mediated by structural change of the target RNA or by binding
358 of a small regulatory RNA, this interaction acting positively or negatively on the stability and
359 translation of the target [43]. For instance, a sRNA-dependent mRNA cleavage of the 5' UTR of
360 *colA* mRNA, which encodes the collagenase in *Clostridium perfringens*, releases a more stable
361 transcript allowing overexpression of the toxin [44]. Several *F. psychrophilum* sRNAs were shown
362 to accumulate in the presence of blood [31] and are regulator candidates for the *bfpR* post-
363 transcriptional regulation. It is also noteworthy that the regulatory event leading to *bfpR*
364 accumulation occurs also under specific conditions without hemoglobin such as in biofilm [45] or
365 in stationary phase [31].

366

## 367 Role of the two heme/hemoglobin receptors in heme acquisition and 368 host colonization

369 For vertebrate pathogens, the most abundant form of iron is bound within heme, and mainly
370 sequestered into hemoglobin in erythrocytes and into other host proteins. In rainbow trout, serum
371 albumin, hemopexin-like proteins and hemoglobin are among the most abundant proteins in plasma
372 [46].

373 *In vitro*, when ferric iron was deprived and heme or hemoglobin was the sole iron source,
374 the growth of *F. psychrophilum* was strongly impaired in the absence of HfpR, but only slowed in
375 the absence of HfpY. The importance of the hemophore was nevertheless obvious *in vivo*, the lack
376 of HfpY resulting in reduced mortality and bacterial loads in spleen. These results indicate that the
377 outer membrane receptor is able to independently capture and transport heme, although cooperation
378 with its cognate hemophore is needed *in vivo*, likely to outcompete the host sequestration systems
379 (Fig 8). The effectiveness of hemophore-based receptors to capture very low levels of heme was
380 exemplified for several acquisition systems, such as the Has system found in *Serratia marcescens*
381 and other Gram-negative bacteria: the affinity of HasR for the hemophore was 100-fold higher than
382 for free heme [47, 48].

383 Direct binding of various substrates to the HfpR receptor was not assayed here, but
384 meaningful information can be deduced from phenotypic results. The Hfp system was able to
385 provide nutrient iron by the uptake of heme from hemoglobin. Previously, it was established that
386 *F. psychrophilum* cells are highly proteolytic and that a T9SS-deficient mutant is unable to
387 consume hemoglobin [21]. This indicates that the Hfp system may require additional factors to
388 efficiently retrieve heme from hemoproteins. We propose that hemoglobin cleavage by
389 exopeptidases contribute to release heme molecules which are then captured by the hemophore
390 HfpY for delivery to the outer membrane receptor. Other hemoproteins such as serum albumin or
391 hemopexin may similarly serve as alternative heme source after their proteolysis by secreted
392 peptidases.

393 The expression profile of *bfpR* and the phenotypic characterization of the corresponding
394 deletion mutant suggested a role in adaptation to hemoglobin overload, a stress condition that the
395 pathogen likely undergoes during its lifecycle (Fig 8). Indeed, infected fish develop hemorrhagic
396 septicemia [13]. *F. psychrophilum* cells are hemolytic and high bacterial load in blood could result
397 in the release of large amounts of hemoglobin. Bacterial cells also accumulate at high level in
398 spleen and kidney, two hematopoietic tissues in teleost fish. In particular, the spleen acts as a filter
399 for blood-derived substances and plays a major role for pathogens clearing and turnover of
400 erythrocytes through phagocytosis by melanomacrophages [49]. This infection niche thus
401 accumulates large amount of heme. We assume that the hemoglobin concentration (1%) used for
402 *in vitro* experiments properly mimics massive hemolysis, as total hemoglobin levels of 6 to 12 %
403 (g/dl) in blood of healthy rainbow trout were reported [50]. The results showed that the presence
404 of 1% hemoglobin did not affect the viability of *F. psychrophilum*, rather, the growth of wild-type
405 was only slightly reduced and the final biomass was increased. In contrast, the lack of BfpR resulted
406 in a greatly reduced growth rate. Under these conditions, the Hfp uptake system was strongly
407 repressed, though free iron was available as nutrient iron source. We concluded that *F.*
408 *psychrophilum* cells can sustain high concentration of hemoglobin (equivalent to 620 µM heme)
409 without toxicity and that BfpR is involved in this adaptation. Several Gram-negative pathogenic
410 bacteria are reported to accumulate heme in their membrane with no apparent toxicity, whereas
411 others are highly susceptible [51]. Additional experiments are ongoing in order to better
412 characterize the function of BfpR in the physiology of *F. psychrophilum* under hemoglobin
413 overload.

414 Experimental infection in rainbow trout fry using intramuscular injection or immersion
415 models highlighted the major contribution of the Hfp system to virulence and host colonization. In
416 contrast, the lack of BfpR had no significant impact on these experiments. It is noteworthy that

417 experimental infection of rainbow trout at the early stage (~1 to 5 g) by strain OSU THCO2-90
418 induced acute mortality 2- to 3-days post-infection, this tiny window making monitoring of the
419 infectious process difficult. We thus infected juvenile rainbow trout (~65 g) which immune system
420 is expected to be more mature, allowing a better resistance against infection. Mortalities occurred
421 between 4- and 8-days post infection with the wild-type, whereas the lack of BfpR resulted both in
422 reduced bacterial loads in blood, spleen and kidney and in increased fish survival. This confirms
423 that BfpR contributes to *in vivo* fitness in *F. psychrophilum*. Overall, we propose that both BfpR
424 and Hfp systems support heme uptake with non-redundant functions and act at distinct substrate
425 concentration ranges to adapt the physiology of *F. psychrophilum* to iron sources available in the
426 surrounding environment. Many pathogenic bacteria evolved to produce multiple heme receptors,
427 each of them contributing to host colonization. For instance, *P. aeruginosa* produces three outer
428 membrane heme receptors: the hemophore-dependent systems HxuA and Has act mostly as sensors
429 of extracellular heme, while the hemophore-independent PhuR receptor ensures the uptake of high
430 amounts of heme providing nutrient iron for growth [52, 53].
431

## 432 Sequence properties of the BfpR and HfpR receptors and the HfpY 433 hemophore

434 Distinct TBDRs typically display similar 3D-structural organization but low-sequence
435 similarity (~20%). Predicting the substrate of TBDRs is challenging as specificity resides more in
436 a few residues located in external loops and internal surface of the channel than in the global
437 sequence conservation of the beta-barrel domain. Despite the high diversity between sequences,
438 conserved amino acid motifs have been identified in heme/hemoglobin receptors characterized in
439 other Gram-negative bacteria [54-56]. Multiple sequence alignments showed that the FRAP/NxxL

440 motifs and the histidine residue located within the external loop L7 in other hemoglobin/heme
441 receptors were conserved in BfpR (F11A in *Supporting Information*), suggesting that it interacts
442 directly with hemoglobin. In the case of HfpR, the loop L7 was extended (78 AA instead of 34 AA
443 for *P. gingivalis* HmuR) and motif conservation was only partial. No obvious conservation of the
444 FRAP/NxxL motifs was found for the two other TBDRs (THC0290_0681 and THC0290_0369)
445 that are overexpressed by low-iron conditions and in the presence of blood, respectively (Fig 1,
446 F11B in *Supporting Information*). These FRAP/NxxL motifs and histidine residue are thought to
447 mediate hemoglobin binding and heme utilization, although mutagenesis studies of *P. gingivalis*
448 HmuR and *Haemophilus ducreyi* HgbA showed a different behavior and other residues can be
449 involved in substrate interaction [54-56].

450 We noticed that, compared to other TonB-dependent hemoglobin receptors, BfpR possesses
451 an additional domain called NTE for N-terminal extension (Carboxypeptidase D regulatory-like,
452 IPR008969) which is frequently found in TBDRs (*i.e.* 16 out of 23 TBDRs in strain OSU THCO2-
453 90). This domain of unknown function may contribute to substrate uptake as recently exemplified
454 for the levan acquisition system in *Bacteroides thetaiotaomicron* [57].

455 The low sequence similarity of BfpR and HfpR with other characterized heme/hemoglobin
456 receptors makes the transfer of knowledge hazardous and future investigations are needed to
457 decipher the heme transport mediated by BfpR and HfpR at the molecular level. Moreover, the
458 very low sequence conservation of HfpY with other members of the HmuY family makes it
459 probable that the hemophore of *F. psychrophilum* functions using an original heme-binding
460 mechanism. Indeed, despite a general conservation of heme binding ability in all five HmuY-like
461 proteins described so far in strict anaerobes (*P. gingivalis, Tannerella forsythia*, *Prevotella*
462 *intermedia* and *Bacteroides vulgatus*), in depth studies revealed important differences in their mode

463 of interaction with heme; for instance, heme coordination involved His134/His166 in *P. gingivalis*
464 HmuY but Met140/Met169 in *T. forthysia* Tfo [35, 58].
465

## 466 Other iron acquisition systems are predicted in the genome of *F.* 467 *psychrophilum*

468 The majority of TBDRs encoded in the *F. psychrophilum* genome have unknown functions.
469 Based on the expression profiles in plasma or blood, several other candidates may also contribute
470 to iron acquisition from heme or other iron sources. Occurrence analysis of TBDR encoding genes
471 in *F. psychrophilum* genomes identified several receptors present only in genomes from specific
472 lineages. Molecular epidemiology studies of *F. psychrophilum* outbreaks revealed an epidemic
473 population structure with limited number of clonal complexes that are associated with host fish
474 species [6, 32]. Phenotypic diversity between isolates was reported and a few related genetic
475 determinants identified so far by comparative genomics [59-65]. Here, we found a gene cluster
476 containing an uncharacterized TBDR-encoding gene (FP2456 in strain JIP 02/86) present only in
477 genomes belonging to the two predominant clonal complexes infecting rainbow trout (*i.e.,* CC-
478 ST10 and CC-ST-90). The FP2456 protein belongs to the TonB-dependent siderophore receptor
479 family (TIGR01783) and genes conserved in synteny encode two putative siderophore biosynthesis
480 enzymes and a MFS-type efflux transporter. Further studies aiming to characterize the role of this
481 predicted siderophore system in iron acquisition and *in vivo* fitness are of great interest but are
482 currently limited by the lack of efficient mutagenesis tools to manipulate these isolates.
483

## 484 Conclusion

485 This study provides molecular knowledge on three novel molecular factors involved in the
486 infection process. The results will help to determine future directions of study for many aspects of
487 heme acquisition. A brief list of interesting topics would be the characterization of regulatory
488 events that coordinate expression of HfpR and BfpR receptors in response to environmental
489 changes and identification of additional proteins involved in the process such as exopeptidases
490 releasing heme from hemoproteins, putative heme oxygenase degrading heme to free ferrous iron,
491 or inner membrane transporter mediating transfer to the cytoplasm. *F. psychrophilum* likely
492 evolved several acquisition strategies to take advantage of the diversity of iron sources encountered
493 during its lifecycle. Mutagenesis of other putative iron acquisition systems may also unveil
494 additional factors favouring host colonisation and disease development. *F. psychrophilum*
495 infections are a major threat for salmonid farming worldwide and innovative control strategies are
496 needed to limit their impact. This study shows that heme outer membrane receptors have a major
497 contribution to bacterial fitness in the fish host and are promising targets for innovative
498 antibacterial strategies [66].
499

500 # Materials and Methods

501 ## Bacterial strains and growth conditions

502 The strains used in this study are listed in T1 in *Supporting Information*. This study was
503 performed using THCO2-90, a model strain for *F. psychrophilum* genetic manipulation [17, 67].
504 *F. psychrophilum* was routinely grown aerobically in tryptone yeast extract salts (TYES) broth [0.4
505 % (w/v) tryptone, 0.04 % yeast extract, 0.05 % (w/v) $MgSO_4$ $7H_2O$, 0.02 % (w/v) $CaCl_2$ $2H_2O$,
506 0.05 % (w/v) D-glucose, pH 7.2] or on TYES agar. When specified, media was supplemented with
507 5% fetal calf serum (FCS) for optimal growth. Growth experiments in liquid culture were carried
508 out at 200 rpm and 18 °C, as follows: strains were streaked on TYES FCS agar from -80°C freezer
509 stock and incubated 4 days at 18°C, a pre-culture was then prepared by inoculation of one colony
510 into 5 ml of TYES broth and incubation during 36 h. Cultures were performed by inoculation of
511 10 ml of broth medium at an OD600 of 0.02 with the pre-culture and growth was evaluated by
512 measuring OD600 using a Biochrom WPA CO8000 spectrophotometer. Iron-depleted cultures
513 were performed in 10 ml of TYES broth supplemented with 20 µM ethylenediamine-*N*,*N'*-bis (2-
514 hydroxyphenylacetic acid) (EDDHA) and 1.25 µM hemoglobin, 5 µM hemin or 5 µM $FeCl_3$ when
515 specified. Stock solutions were prepared as follows: 2.5 mM lyophilized hemoglobin (Sigma
516 #H2500) in 0.1 M Tris 0.14 M NaCl, 10 mM hemin chloride (Fe-PPIX) (Frontier Scientific) in 50
517 mM NaOH, 50 mM $FeCl_3$ (Merck) in water and 25 mM EDDHA (Sigma) in 50 mM NaOH.
518 Hemoglobin-enriched cultures were performed by inoculation of the pre-culture at an OD600 of
519 0.005 into 5 ml of TYES broth supplemented with 1% hemoglobin (w/v) prepared from a fresh
520 10% hemoglobin (Sigma #08449) stock solution. Growth curves were determined by enumeration
521 of colony-forming units (CFU) by plating serial dilutions of the cultures on TYES FCS agar plates.
522 The elastin degradation assay was performed using TYES agar supplemented with 0.75 % (w/v)

523 elastin from bovine neck ligament (Sigma, E1625) as previously described [64]. *E. coli* strains
524 were grown at 37°C in Luria Bertani broth or supplemented with 15 g/l of agar.
525

## 526 Bioinformatic analysis

527 Comparison of the gene content between strains was performed on a selection of 22
528 genomes using the web interface MicroScope [68]. TBDR encoding genes were identified using
529 Interpro predictions of the TonB-dependent receptor family (IPR000531) or the highly conserved
530 structural beta-barrel (IPR036942) and plug (IPR037066) domains. Orthologs were identified
531 using BlastP Bidirectional Best Hit and the MicroScope default parameters (i.e., >80% protein
532 identity, >80% coverage). The presence of truncated TBDR genes was verified by PCR and Sanger
533 sequencing. The structure-assisted multiple sequence alignments of HfpR (THC0290_1814) and
534 BfpR (THC0290_1679) with other heme/hemoglobin receptors and of HfpY (THC0290_1812)
535 with other HmuY-like proteins were constructed with PROMALS3D [69] webserver.
536

## 537 Plasmid construction and conjugative transfer into *F. psychrophilum*

538 Plasmids (T1 in *Supporting Information*) were engineered by the Gibson assembly method
539 using the NEBuilder® HiFi DNA Assembly Master Mix (New England Biolabs) with appropriate
540 primers (T3 in *Supporting Information*). Plasmids were constructed in *E. coli* DH5α Z1, verified
541 by PCR and DNA sequencing, transferred to *E. coli* MFD*pir* and subsequently introduced into *F.*
542 *psychrophilum* OSU THCO2-90 by conjugation as previously described [31]. For selective growth
543 of *E. coli* strains carrying plasmids, transformants were selected with 100 µg/ml of ampicillin.
544 Cultures of *E. coli* MFD*pir* were supplemented with 0.3 mM diaminopimelic acid (Sigma-Aldrich

545 Co.). Selection of *F. psychrophilum* transconjugants was carried out with 50 µg/ml of gentamycin
546 and 10 µg/ml of erythromycin for the pCP*Gm*$^{r}$- and pYT313-derivative plasmids, respectively.
547

## 548 Construction of transcriptional reporter plasmids and promoter 549 activity monitoring

550 pCP*Gm*$^{r}$-$P_{less}$-mCh derivative plasmids carrying the promoter region upstream of *hfpR* (240
551 bp) or *bfpR* (various length: 306, 609 and 950 bp) were constructed as previously described [31].
552 Briefly, the vector fragment was amplified using primers TRO460/TRO461 with pCP*Gm*$^{r}$-$P_{less}$-
553 mCh as matrix and the promoter region using strain OSU THCO2-90 chromosomal DNA and either
554 primers TRO462/TRO463 resulting in $P_{hfpR}$-mCh fusion (pGi48), TRO464/TRO465 resulting in
555 $P_{bfpR_1}$-mCh (306 bp, pGi49), TRO789/TRO790 resulting in $P_{bfpR_2}$-mCh (609 bp, pGi74) or
556 TRO824/TRO790 resulting in $P_{bfpR_3}$-mCh (950 bp, pGi80) fusions. For promoter activity
557 monitoring of $P_{hfpR}$-mCh fusion, log-phase cultures (OD600 of 0.4) of the strain carrying the pGi47
558 plasmid performed in TYES broth supplemented with 20 µg/l gentamycin were distributed into 96-
559 well microtiter plate, cultures were then supplemented with 20 µM of the iron chelator EDDHA
560 and various iron sources (62.5 µM hemoglobin, 250 µM hemin, 5 to 250 µM $FeCl_3$) and incubated
561 with continuous shaking at 18°C during 5 h. Cultures of strain carrying the pCP*Gm*$^{r}$-$P_{less}$-mCh
562 plasmid were used as negative control. Promoter activity monitoring of $P_{bfp}$-mCh fusions was
563 performed using bacterial colonies grown during 48 h on TYES agar supplemented with 1 %
564 hemoglobin or not. Colonies were scraped from the plates, then resuspended in TYES broth at a
565 final OD600 of 1 for fluorescence measurement. Expression of the *mcherry* gene was monitored
566 using whole-cell fluorescence with a Tecan Microplate Reader (Infinite 200 PRO). Excitation and

567 emission wavelengths were set at 535 nm and 610 nm, respectively. Promoter activity (in arbitrary
568 units) was estimated by dividing fluorescence intensity by the OD600.
569

## 570 Construction of *F. psychrophilum* mutants

571 Three suicide vectors pGi27, pGi29 and pGi38 allowing, respectively, *hfpR*, *hfpY* and *bfpR*
572 deletion were constructed using the pYT313 plasmid [70] as previously described (M1 in
573 *Supporting Information*)[31]. Each resulting plasmid was introduced by conjugation in strain OSU
574 THCO2-90 and colonies selected for double crossing-over were screened by PCR using specific
575 primers (T3 in *Supporting Information*) in order to identify those carrying the deletion genotype.
576 The THC0290_1813 transposition mutant was produced as part of a Tn*4351* mutant library as
577 previously described [23, 71]. Briefly, the pEP4351 suicide plasmid carrying Tn*4351* was
578 introduced by conjugation in strain OSU THCO2-90 and clones were selected on TYES agar
579 supplemented with 10 µg/l erythromycin. Identification of the Tn*4351* interrupted locus was
580 performed by digestion of genomic DNA by HindIII, ligation, inverse PCR of the resulting circular
581 molecules using primers targeting Tn*4351* and subsequent sequencing of the amplicons. Sequences
582 were used to locate the transposon insertion site into the genomic sequence.
583

## 584 Construction of a *F. psychrophilum* chromosomal expression 585 platform

586 Several suicide plasmids allowing chromosomal recombination and gene insertion at a
587 neutral intergenic region (between genomic positions 1121879 and 1124880 for strain OSU
588 THCO2-90) were constructed using pYT313 as backbone (T1 in *Supporting Information*). pGi39
589 was designed to carry the two DNA fragments upstream and downstream of the insertion site

590 flanking an expression platform composed of a constitutive promoter $P_{rpsL}$, a multiple cloning site
591 and an intrinsic terminator, and pGi42 to carry the elastase encoding gene FP0506 under the control
592 of $P_{rpsL}$ (M2 in *Supporting Information*).
593

## 594 Complementation of the deletion mutants

595 The chromosomal ectopic platform was used for reintroduction of deleted genes into the
596 mutant strains. A set of pGi39-derivative plasmids (pGi44, pGi45, pGi46 and pGi55; T1 in
597 *Supporting Information*) was constructed and introduced by conjugation in the respective mutant
598 strains, resulting in the chromosomal insertion of a single copy gene under the control of native
599 promoter at the neutral intergenic region (M2 and F2 in *Supporting Information*).
600

## 601 Recombinant MBP-HfpY purification and heme binding assays

602 Recombinant HfpY was purified as a MBP-HfpY fusion protein from the pMBP-HfpY
603 plasmid in *E. coli* Top10. pMBP-HfpY was constructed by gene synthesis (Proteogenix). MBP-
604 HfpY was purified by affinity chromatography on amylose resin as reported previously [72].
605 Briefly, bacteria were grown in 1 L LB broth to OD600 = 0.6 and expression was induced with 0.5
606 mM isopropyl 1-thio-β-D-galactopyranoside (IPTG) overnight at RT. Cells were pelleted at 3500
607 g for 10 min, resuspended in 20 mM Hepes pH 7.5, 300 mM NaCl, containing 1 mM EDTA
608 (binding buffer), and disrupted with glass beads (FastPrep, MP Biomedicals). Cell debris were
609 removed by centrifugation at 18,000 g for 15 min at 4°C. MBP-tagged proteins contained in the
610 supernatant were purified by amylose affinity chromatography (New England Biolabs) following
611 manufacturer's recommendations: the soluble fraction was mixed with amylose resin and incubated
612 on a spinning wheel at 4°C for 1 h. The resin was then centrifuged, and washed 3 times with binding

613 buffer. Purified proteins were eluted in binding buffer containing 10 mM maltose, and dialyzed
614 against 20 mM Hepes pH 7.5, 300 mM NaCl. Quantity and purity of the eluted fraction were
615 determined with the Lowry Method (Biorad) and by SDS-PAGE followed by Coomassie staining,
616 respectively. Heme binding was studied by UV-visible spectroscopy of MBP-HfpY in the presence
617 of hemin in a microplate spectrophotometer (Spark, Tecan).
618

## 619 Titration of MBP-HfpY with hemin

620 Hemin binding affinity and stoichiometry to MBP-HfpY were determined by adding 0.5 to
621 1 µl increments of a 200 µM hemin solution to cuvettes containing 100 µl test samples of 20 µM
622 MBP-HfpY in 20 mM Hepes pH 7.5, 300 mM NaCl, or reference sample without protein. Spectra
623 were measured from 230 nm to 750 nm in a UV-visible spectrophotometer Tecan (Spark). $OD_{398nm}$
624 was plotted against hemin concentration and data were fitted to a one-binding site model (with
625 calculated extinction coefficient of bound hemin of ε398 = 40 $mM^{-1}.cm^{-1}$) as described [72].
626

## 627 Total RNA extraction

628 Bacterial cells from 2 mL cultures were collected by centrifugation for 3 min after addition
629 of ½ volume of frozen killing buffer (20 mM Tris-HCl pH 7.5, 5 mM $MgCl_2$, 20 mM $NaN_3$) to the
630 culture sample. The cell pellets were frozen in liquid nitrogen and stored at −80 °C. For experiments
631 performed in iron-depleted conditions, RNAs were extracted from pellets harvested at an OD600
632 of 0.8. For experiments performed in 1% hemoglobin-enriched conditions, RNAs were extracted
633 from pellets harvested when bacterial concentration reached $10^9$ CFU/ml. Experiments were
634 carried out from three independent cultures per biological condition. The ZymoBIOMICS RNA
635 Miniprep Kit (Zymo Research) was used for total RNAs extraction. 5 µg of RNA extracts were

636 treated using DNase I (Qiagen) to remove residual genomic DNA then purified using the
637 ZymoBIOMICS RNA Miniprep Kit. The RNA concentration was measured using a NanoDrop
638 1000 Spectrophotometer (NanoDrop Technologies, Inc.) and quality was assessed by
639 electrophoresis on denaturing formaldehyde agarose gel.
640

641 **Reverse Transcription PCR**

642 Transcriptional structure of the *bfpR* locus was determined by overlapping RT-PCR
643 experiments. Total RNA was extracted from bacterial pellets harvested from cultures performed in
644 TYES 1 % hemoglobin. cDNA synthesis was carried out on 500 ng of DNase-treated RNA using
645 the SuperScript™ II Reverse Transcriptase (Thermo Fisher) with random primers. Negative control
646 reaction was run under similar conditions except that the reverse transcriptase was omitted (no RT).
647 Polycistronic structure was detected by PCR amplification using cDNA as matrix and several
648 primer sets designed to overlap adjacent genes (TRO677/TRO676 between the upstream region of
649 *bfpR* and its coding sequence, TRO674/TRO675 for the junction between THC0290_1678 and
650 *bfpR,* and TRO672/TRO673 for the junction *asd*-THC0290_1678; T3 in *Supporting Information*).
651 Negative and positive controls were run using no RT cDNA reaction and genomic DNA as matrix,
652 respectively, and results were visualized by electrophoresis of PCR products on 1% agarose gel.
653

654 **Real Time quantitative PCR**

655 cDNA was generated from 500 ng of total RNA in a thermal cycler (Eppendorf) using the
656 iScript™ Advanced cDNA Synthesis Kit for RT-qPCR (BIO-RAD) as recommended by suppliers.
657 cDNA was diluted 1:25 in water and mixed with iTaq Universal SYBR Green Supermix (BIO-
658 RAD) and forward and reverse primers with final concentration at 0.5 µM each. qPCR was

659 performed using a Realplex Mastercycler (Eppendorf) or CFX system (BIO-RAD) with initial
660 denaturation at 95°C for 3 min followed by 40 cycles of amplification as following: denaturation
661 at 95°C for 5 s, annealing and extension at 60°C for 30 s. For each biological replicate, mean Ct
662 values were calculated based on technical triplicate reactions and then normalized using the
663 geomean of Ct values of two reference genes (*rpsA* and *frr*). Relative quantification of mRNA was
664 expressed as $2^{-\Delta\Delta Ct}$ using TYES as a reference sample.
665

## 666 Circular Rapid Amplification of cDNA ends (RACE)

667 RACE was carried out using a general four-step protocol which enables the simultaneous
668 cloning of 5' and 3' ends of RNA, as previously described [73]. Two RNA samples extracted from
669 culture of the wild-type strain performed in TYES broth with 20 µM EDDHA or 1% hemoglobin
670 were used respectively for *hfp* or *bfpR* mRNAs RACE experiments. Briefly, 8 µg of DNase-treated
671 RNA samples were treated by 80 units of RppH (New England Biolabs) at 37°C for 1 hour to
672 transform 5'-triphosphate groups carried by primary transcripts into 5'-monophosphate groups,
673 then purified using the ZymoBIOMICS RNA Miniprep Kit. Circular ligation was performed by
674 adding 80 units of T4 RNA ligase 1 (New England Biolabs) to 4 µg of the RppH-treated sample,
675 the mix was incubated at 16°C overnight then heat inactivated. A control sample was prepared
676 following the same protocol except that RppH was omitted in the reaction. First strand cDNA
677 synthesis was performed using the SuperScript™ II Reverse Transcriptase (Thermo Fisher) with
678 400 ng of the ligation product as the matrix and a specific primer for each 3'-5' cDNA. 5'-3' ends
679 junctions were then amplified by PCR using cDNA as the matrix and specific primers (T3 and F4
680 in *Supporting Information*). PCR products were cloned into the pJET1.2 vector using the CloneJET
681 PCR Cloning Kit (Thermo Fisher) then introduced in *E. coli*. Colonies were screened by PCR prior

682 Sanger sequencing of the insert. Three 3'-5' cDNAs carrying *hfpR*, *hfpY* or *bfpR* were produced
683 using the gene-specific primers TRO806, TRO811 or TRO814, respectively. Detection of mRNA
684 boundaries was performed as follows: for the *hfpR* cDNA using primers TRO806/TRO807
685 amplifying *hfpR*-THC0290_1813-*hfpY* mRNAs, for the *hfpY* cDNA using primers
686 TRO812/TRO807 amplifying all *hfpY* mRNAs and for the *bfpR* cDNA using three sets of primers
687 amplifying either all *bfpR* mRNAs (TRO815/TRO816), THC0290_1678-*bfpR* mRNAs
688 (TRO815/TRO825) or *asd*-THC0290_1678-*bfpR* mRNAs (TRO815/TRO827). For *bfpR* RACE
689 experiments, the first PCRs were followed by a nested PCR using TRO817/TRO818,
690 TRO817/TRO826 or TRO817/TRO828, respectively, and the resulting PCR products were cloned
691 into the pJET1.2 vector for Sanger sequencing.
692

693 **Rainbow trout experimental infections**

694 Three experimental infections models were used in this study differing in the infection route
695 (intramuscular injection *versus* immersion), the rainbow trout lines or the size of fish (fry *versus*
696 juvenile fish). Fish were reared at 10°C in recycling aquaculture system (RAS) with dechlorinated
697 water, then transferred to BSL2 zone in tanks in flow water (1 renewal per hour) for infection
698 experiments.

699 For the intramuscular injection model at the fry stage, fish (average body weight of 5 g) of
700 the rainbow trout standard line (Sy*Aut) selected by INRAE were used. Six groups of 10 fish were
701 anesthetized and challenged with the wild-type strain at different doses, as follows: 6 bacterial
702 suspensions were prepared by ten-fold serial dilution of a culture at an OD600 of 1 performed in
703 TYES broth, and 50 µl of each suspension was injected per fish, corresponding to 50 CFU to 5 x
704 $10^6$ CFU. LD50 of the wild-type was estimated at 5 x $10^6$ CFU. A similar procedure was used for

705 the 8 deletion mutants and complemented strains except that only 3 doses were tested,
706 corresponding to 5 x $10^4$ CFU, 5 x $10^5$ CFU and 5 x $10^6$ CFU per fish. *F. psychrophilum* bacterial
707 counts were determined by plating serial dilutions of bacterial suspensions on TYES agar
708 supplemented with FCS. After injection, fish were maintained in flow-through water at 10°C and
709 mortalities were recorded twice a day for two weeks.

710 The ability of bacterial strains to colonize rainbow trout at the fry stage (average body
711 weight of 2 g) was compared using the bath infection model on the rainbow trout homozygous line
712 A36, which is highly susceptible to *F. psychrophilum* infection [10, 23, 74]. Groups of 40 fish in
713 duplicates were used for each strain. Bacterial cultures were prepared as follows: two independent
714 cultures of the wild-type, deletion and complemented mutant strains were grown in TYES broth
715 until late-exponential phase (OD600 of 1). The bacterial cultures were directly diluted (200-fold)
716 into 10 l of aquarium water. Bacteria were maintained in contact with fish for 24 h by stopping the
717 water flow and were subsequently removed by restoring the flow. During the experiment, water
718 was maintained at 10°C under continuous aeration and physical parameters ($NH_4^+$, $NO_2^-$) were
719 monitored. Sterile TYES broth was used for the control group. *F. psychrophilum* bacterial counts
720 were determined at the beginning and at the end of the immersion challenge by plating serial
721 dilutions of water sample on TYES FCS agar. Five fish from each tank (n = 10 per strain) were
722 randomly chosen and euthanatized (tricaine, 300 mg/l) at 6 h post-infection to sample gills and
723 spleen. Organs were mechanically disrupted in tubes containing 400 µl of peptone (10 g/l water)
724 and 1 mm ceramic beads (Mineralex SAS, Lyon, France) using a FastPrep-24™ 5G instrument at
725 6.0 m s-1 for two cycles of 20 s (MP Biomedicals), and bacterial loads were determined by plating
726 serial dilutions of lysates on TYES FCS agar.

727 Virulence of the *bfpR* deletion mutant and the wild-type strain was evaluated by
728 intramuscular injection at the juvenile stage (average body weight of 65 ± 9 g) using the rainbow

729 trout line A36. Bacterial suspension was prepared by 10-fold dilution in sterile TYES of a culture
730 at an OD600 of 1. For each strain, a group of 24 fish were anesthetized and inoculated with 100 µl
731 of bacterial suspension then maintained in flow-through water at 10°C into two compartments: the
732 first subset (n = 10) was used for survival estimation by recording mortalities during 2 weeks and
733 the second subset (n = 12) for sampling of spleen, head kidney and blood at 4 days post-infection
734 and bacterial loads determination. Following anesthesia, blood (150 µL per fish) was collected
735 from the caudal vein using syringes containing heparin (500 units/ml) and the bacteremia was
736 determined by plating fresh blood and serial dilutions on TYES FCS agar plates. Infectious doses
737 and bacterial loads in organs were determined as described above.

738 Statistical differences of bacterial loads between groups were analyzed using the Mann-
739 Whitney test, and survival curves were determined using the Kaplan-Meier method and compared
740 using the Mantel-Cox log-rank test with GraphPad Prism 8.2.0 (GraphPad Software, San Diego,
741 CA, USA).

## 742 Ethics statements

743 The infection challenges were conducted at the INRAE-IERP Fish facilities of Jouy-en-
744 Josas (building agreement n°C78-720), performed in accordance with the European Directive
745 2010/2063/UE regarding animal experiments, and approved by the institutional review ethics
746 committee, COMETHEA, of the INRAE Center in Jouy-en-Josas, France. Authorizations were
747 approved by the Direction of the Veterinary Services of Versailles (authorization number #19210-
748 2015100215242446).

749

# Acknowledgements

The authors are grateful to the staff of the fish facilities (IERP, INRAE, 2018. Infectiology of fishes and rodent facility, doi: 10.15454/1.5572427140471238E12 and PEIMA, INRAE, Fish Farming Systems Experimental Facility, doi: 10.15454/1.5572329612068406E12), to Edwige Quillet and Nicolas Dechamp (INRAE GABI, France) for supplying fish and advice, and to Benjamin Fradet and Claire Gautier-Brossois for technical assistance. We thank Elise Borezée-Durant, Alexandra Gruss, Rodrigo Coronel-Tellez, Philippe Bouloc and Mirjam Czjzek for helpful discussions. This work has benefited from the MicroScope annotation platform for computational resources.


# Supporting information

**Supporting Information.pdf** This file contains Supplementary Methods (M1 to M3), Supplementary Figures (F1 to F11) and Supplementary Tables (T1 to T3).

763 # Figure legends

764 **Fig 1. Conservation and gene expression of the 24 TonB-dependent receptors encoded in the**
765 **genome of strain OSU THCO2-90.** (A) *In silico* prediction of TBDR encoding genes. The list of
766 TBDR encoding genes was retrieved by *in silico* prediction of the plug and ß-barrel domains.
767 Conservation in a selection of 22 isolates: gene present (blue), truncated (grey), absent (white).
768 [(a)]MLST and genomic data are from Duchaud *et al* [32]. CC-ST: clonal complex-sequence type.
769 [(b)]Fish host: *Oncorhynchus mykiss*, *Salmo trutta*, *Tinca tinca*, *Gasterosteus aculeatus*, *Plecoglossus*
770 *altivelis*, *Oncorhynchus kitsutch*, *Salmo salar.* (B) TBDR-encoding genes significantly upregulated
771 (green) and down-regulated (red) in strain OSU THCO2-90 in iron-limited condition (TYES + 25
772 µM 2,2'-dipyridyl), under rainbow trout plasma exposure or in the presence of blood (TYES agar
773 supplemented with 10% horse blood). Differential expression is expressed as log2-fold change
774 values retrieved from Guérin *et al* [31](https://fpeb.migale.inrae.fr).

775 **Fig 2. Transcriptional organization of the *bfpR* locus and its regulation by hemoglobin**
776 **concentration.** (A) Genomic view of the *bfpR* locus, microarray expression profiles and putative
777 transcription start sites (TSS) from Guérin *et al* [31]. Expression profiles (log2-expression signal)
778 show the upregulation of *bfpR* in the presence of blood: bacterial colonies grown on TYES agar
779 (TYESA) covered by 10% defibrinated horse blood (violet) or not (black). 3'-5' RACE: Schematic
780 representation of 5' and 3' ends identified by circular 3'-5' RACE experiments. Positions of the 5'
781 and 3' ends are relative to the start and stop positions of *bfpR* CDS, respectively. (B) Assessment
782 of transcriptional initiation upstream of *bfpR* using transcriptional fusions. Promoter activity was
783 measured using whole-cell fluorescence of *F. psychrophilum* cells carrying the reporter plasmid
784 pCPGm$^{r}$-P$_{less}$-mCh with various DNA fragments (P$_{less}$: empty plasmid; P*bfpR*_1: 306 bp, P*bfpR*_2:
785 609 bp, P*bfpR*_3: 950 bp). Bacterial colonies were grown on TYES agar supplemented with 1%

786 hemoglobin (equivalent of 620 µM heme molecules) or not. Values represent the mean and
787 standard deviation of three independent experiments. (*) indicates significant difference identified
788 in a two-way ANOVA analysis (Bonferroni adjusted p-value < 0.05). (C) RT-qPCR measurement
789 of *bfpR* expression. mRNA level was quantified using RNA extracted from cultures performed in
790 TYES broth supplemented with 1% hemoglobin (Hb 1%) or not. Ct values of genes were
791 normalized using the geomean of two reference genes (*rpsA* and *frr)*. RQ: Relative quantification
792 of mRNA was expressed as $2^{-\Delta\Delta Ct}$ using TYES as reference sample. Values are the mean and
793 standard deviation of three independent experiments.

794 **Fig 3. *bfpR* is required for *in vitro* growth under high hemoglobin concentration.** Growth under
795 high hemoglobin concentration determined by viable cell measurements (CFU/mL) of cultures in
796 TYES broth supplemented with 1% hemoglobin. Plain lines: wild-type (black) and deletion
797 mutants (Δ*bfpR*: green; Δ*hfpR*Δ*bfpR*: brown), dashed lines: ectopic complemented mutants. Values
798 represent the mean and standard deviation of four independent experiments.

799 **Fig 4. Transcriptional organization of the *hfp* locus and its regulation by iron availability.** (A)
800 Genomic view of the *hfpR*-THC0290_1813-*hfpY* locus, microarray expression profiles and putative
801 TSSs from Guérin *et al* [31] are shown (see legend of Fig 2). For iron limitation, cells were grown
802 in TYES broth supplemented with 25 µM 2,2'-dipyridyl (red) or not (black); for blood
803 supplementation, cells were from colonies grown on TYES agar (TYESA) covered by 10%
804 defibrinated horse blood (violet) or not (black). 3'-5' RACE: Schematic representation of 5' and
805 3' ends identified by circular 3'-5' RACE experiments. Positions of the two 5' ends and of the 3'
806 end are relative respectively to start positions of *hfpR*, *hfpY*, and stop position of *hfpY*. (B)
807 Transcriptional regulation of the *hfpR* promoter by iron availability. Promoter activity was
808 measured using whole-cell fluorescence of the wild-type strain carrying the reporter plasmid with

809 240 bp DNA upstream of *hfpR* ($P_{hfpR}$). Bacteria were grown in iron depleted TYES broth (E20, 20
810 μM EDDHA) supplemented with a range of $FeCl_3$ (upper panel) or with different iron sources
811 (lower panel) as indicated. Cultures were inoculated at OD600 0.4 and fluorescence was measured
812 during 5 h as described in Materials and Methods. Strain carrying the empty plasmid ($P_{less}$) was
813 used as control. Values represent the mean and standard deviation of three independent experiments.
814 (C) *hfpR*, *1813* and *hfpY* mRNA levels correlate with iron availability. RT-qPCR measurements
815 were performed under iron depletion (upper panel) or high concentration of hemoglobin (lower
816 panel) as described in Fig 2 using the wild-type strain grown in TYES broth, iron-depleted TYES
817 (E20) supplemented with 1.25 μM hemoglobin (E20 Hb) or in TYES supplemented with 1%
818 hemoglobin (Hb 1%).

819 **Fig 5. *hfpR* is required for *in vitro* growth under iron scarcity.** Growth measured by optical
820 density at 600nm of the wild-type, mutants and complemented strains (rows) under various
821 conditions of iron availability (columns). Cultures were performed in TYES broth containing the
822 iron chelator EDDHA 20 μM only (circle) or containing EDDHA and an iron source (triangle):
823 1.25 μM hemoglobin (left); 5 μM hemin (center) and 5 μM $FeCl_3$ (right). Growth curves in TYES
824 broth were similar for all strains and are plotted for the WT panel only (diamond). Plain lines: wild-
825 type and deletion mutants (Δ*hfpR*: red, Δ*hfpY*: blue, Δ*bfpR*: green, Δ*hfpR*Δ*bfpR*: brown), dashed
826 lines: ectopic complemented mutants. For mutants, growth curves of wild-type are in light grey for
827 comparison purpose. Values represent the mean and standard deviation of three independent
828 experiments. Growth with different iron sources were from independent experiments.

829 **Fig 6. HfpY is a heme-binding protein.** (A) UV-visible absorption spectra of MBP-HfpY
830 complexed with hemin. 40 μM MBP-HfpY was purified from *E. coli* and mixed with equimolar
831 concentration of hemin. UV-visible spectra (in 200 μl) of the complex and same concentration of

832 hemin were obtained in a microplate spectrophotometer (Spark; Tecan). (Inset) 5X Magnification
833 of the 500- to 700 nm region. Results are representative of three independent experiments. (B)
834 Titration of MBP-HfpY with hemin followed by absorbance at 398 nm. 20 μM of MBP-HfpY were
835 mixed with increasing concentrations of hemin as indicated. For each spectrum, the absorbance of
836 the same concentration of hemin was subtracted and the difference absorption spectra are shown,
837 from light to dark blue color as a function of hemin concentration. The absorption difference at
838 398 nm was plotted against hemin concentration (Inset). The curve is representative of 3
839 independent experiments and was fitted using the nonlinear regression function of GraphPad Prism
840 4 software, which determined that the stoichiometry of the HfpY-hemin complex was 1:1.

841 **Fig 7. Evaluation of the virulence of wild-type and deletion mutant strains in rainbow trout.**
842 (A) Bacterial loads in the spleen of rainbow trout fry after immersion challenge (A36 line, 2 g
843 average weight). Each tank was inoculated at a bacterial concentration of 1 (±0.3) x $10^7$ CFU/mL
844 and fish were maintained in contact with bacteria for 24 h at 10°C under optimal oxygenation
845 conditions. At the end of the challenge, bacterial concentration in water was 2 (±0.7) x $10^7$ CFU/mL.
846 Ten fish from each group were sacrificed at 6 h post-infection and bacterial loads in the spleen
847 were determined. Horizontal dashed line indicates the detection threshold. Values are significantly
848 lower in the spleen of groups infected with the Δ*hfpR* and Δ*hfpY* mutants compared to the wild-
849 type and complemented strains (Mann-Whitney: *, 0.033; **, 0.002; ***, <0.001). (B) Kaplan-
850 Meier survival curves of rainbow trout fry (Sy*Aut line, 5 g average weight) after intramuscular
851 injection. Each group (n=10) was challenged at a dose corresponding to 10 x LD50 of the wild-
852 type strain. Upper panel: 3 x $10^6$ CFU for the wild-type (black), 2 x $10^6$ CFU for Δ*hfpR* (red plain
853 line) and ecto::*hfpR* (red dashed line); lower panel: 6 x $10^6$ CFU for the wild-type, 7 x $10^6$ CFU for
854 Δ*hfpY* (blue plain line) and ecto::*hfpY* (blue dashed line). The survival curves for fish inoculated

855 with either the wild-type or the ectopic complemented mutants were significantly different from
856 those inoculated with the Δ*hfpR* or Δ*hfpY* mutants (p-value of the Mantel-Cox log-rank test is
857 indicated). (C-D) Experimental infection of juvenile rainbow trout (A36 line, 65 g average weight)
858 after intramuscular injection. Fish were inoculated with 1 x $10^7$ CFU for the wild-type (black) or
859 Δ*bfpR* mutant (green) strains; a subset (n = 12) was used for bacterial loads determination in blood,
860 spleen and head kidney at 4 days post-infection (C) and another subset (n = 12) for survival
861 estimation (D). Significant differences were observed between both the Kaplan-Meier survival
862 curves (Mantel-Cox log-rank test p-value) and the bacterial loads (Mann-Whitney test).

863 **Fig 8. Graphical model of non-redundant heme/hemoglobin uptake systems of *F.***
864 ***psychrophilum.*** This study showed that HfpR and BfpR outer membrane receptors both mediate
865 heme uptake, but lack functional redundancy. We propose that HfpR and BfpR act in distinct
866 environmental conditions during pathogenesis. During the early phase of infection, *F.*
867 *psychrophilum* encounters low iron conditions due to the sequestration of essential nutrients by the
868 host; iron is either bound to proteins or complexed in heme-binding proteins [26]. The Hfp system
869 is upregulated in low iron and mediates iron acquisition from heme or hemoglobin (Hb); our results
870 indicate that the HfpY hemophore identified here outcompetes host sequestration systems. In
871 contrast, BfpR is up-regulated in the presence of high amounts of hemoglobin from blood, an iron
872 source available upon massive lysis of erythrocytes (RBC) during late stages of septicemia. In these
873 conditions, the Hfp system is strongly repressed and BfpR may mediate heme uptake by direct
874 binding to hemoglobin. The importance of BfpR for full virulence was observed in juvenile
875 rainbow trout but not in fry. Altogether, these results suggest that *F. psychrophilum* evolved two
876 heme acquisition systems to adapt to the range of substrate concentrations encountered during the
877 infection process as well as to the physiological changes occurring during the life cycle of fish.

# REFERENCES


1. FAO, editor The state of world fisheries and aquaculture 2020. Sustainability in action.2020; Rome, Italy: Food and Agriculture Organization (FAO).
2. Bernardet JF. *Flavobacteriaceae*. Bergey's Manual of Systematics of Archaea and Bacteria 2015.
3. Nematollahi A, Decostere A, Pasmans F, Haesebrouck F. *Flavobacterium psychrophilum* infections in salmonid fish. Journal of fish diseases. 2003;26(10):563-74. Epub 2003/12/05. PubMed PMID: 14653314.
4. Avendano-Herrera R, Tapia-Cammas D, Duchaud E, Irgang R. Serological diversity in *Flavobacterium psychrophilum*: A critical update using isolates retrieved from Chilean salmon farms. Journal of fish diseases. 2020;43(8):877-88. Epub 2020/06/23. doi: 10.1111/jfd.13199. PubMed PMID: 32567047.
5. Fujiwara-Nagata E, Chantry-Darmon C, Bernardet JF, Eguchi M, Duchaud E, Nicolas P. Population structure of the fish pathogen *Flavobacterium psychrophilum* at whole-country and model river levels in Japan. Veterinary research. 2013;44:34. Epub 2013/05/21. doi: 10.1186/1297-9716-44-34. PubMed PMID: 23682575; PubMed Central PMCID: PMC3660162.
6. Nicolas P, Mondot S, Achaz G, Bouchenot C, Bernardet JF, Duchaud E. Population structure of the fish-pathogenic bacterium *Flavobacterium psychrophilum*. Applied and environmental microbiology. 2008;74(12):3702-9. Epub 2008/04/22. doi: 10.1128/AEM.00244-08. PubMed PMID: 18424537; PubMed Central PMCID: PMC2446562.
7. Nilsen H, Sundell K, Duchaud E, Nicolas P, Dalsgaard I, Madsen L, et al. Multilocus sequence typing identifies epidemic clones of *Flavobacterium psychrophilum* in Nordic countries. Applied and environmental microbiology. 2014;80(9):2728-36. Epub 2014/02/25. doi: 10.1128/AEM.04233-13. PubMed PMID: 24561585; PubMed Central PMCID: PMC3993282.
8. Knupp C, Wiens GD, Faisal M, Call DR, Cain KD, Nicolas P, et al. Large-scale Analysis of *Flavobacterium psychrophilum* MLST Genotypes Recovered From North American Salmonids Indicates Both Newly Identified and Recurrent Clonal Complexes are Associated with Disease. Applied and environmental microbiology. 2019. Epub 2019/01/20. doi: 10.1128/AEM.02305-18. PubMed PMID: 30658978.
9. Castillo D, Christiansen RH, Dalsgaard I, Madsen L, Middelboe M. Bacteriophage resistance mechanisms in the fish pathogen *Flavobacterium psychrophilum*: linking genomic mutations to changes in bacterial virulence factors. Applied and environmental microbiology. 2015;81(3):1157-67. Epub 2014/12/07. doi: 10.1128/AEM.03699-14. PubMed PMID: 25480749; PubMed Central PMCID: PMC4292493.
10. Fraslin C, Quillet E, Rochat T, Dechamp N, Bernardet JF, Collet B, et al. Combining Multiple Approaches and Models to Dissect the Genetic Architecture of Resistance to Infections in Fish. Frontiers in genetics. 2020;11:677. Epub 2020/08/06. doi: 10.3389/fgene.2020.00677. PubMed PMID: 32754193; PubMed Central PMCID: PMCPMC7365936.
11. Gomez E, Mendez J, Cascales D, Guijarro JA. *Flavobacterium psychrophilum* vaccine development: a difficult task. Microbial biotechnology. 2014;7(5):414-23. Epub 2014/07/25. doi: 10.1111/1751-7915.12099. PubMed PMID: 25056179; PubMed Central PMCID: PMC4229322.
12. Wiens GD, Lapatra SE, Welch T, Evenhuis JP, Rexroad CE, 3rd, Leeds TD. On-farm performance of rainbow trout (*Oncorhynchus mykiss*) selectively bred for resistance to bacterial cold water disease: Effect of rearing environment on survival phenotype. Aquaculture. 2013;388-391:128-36.
13. Barnes ME, Brown ML. A review of *Flavobacterium psychrophilum* biology, clinical signs, and Bacterial Cold Water Disease prevention and treatment. The Open Fish Science Journal. 2011;4:1-9.
14. Decostere A, D'Haese E, Lammens M, Nelis H, Haesebrouck F. *In vivo* study of phagocytosis, intracellular survival and multiplication of *Flavobacterium psychrophilum* in rainbow trout, *Oncorhynchus mykiss* (Walbaum), spleen phagocytes. Journal of fish diseases. 2001;24:481-7. doi: 10.1046/j.1365-2761.2001.00322.x.
15. Evensen O, Lorenzen E. An immunohistochemical study of *Flexibacter psychrophilus* infection in experimentally and naturally infected rainbow trout (*Oncorhynchus mykiss*) fry. Diseases of aquatic organisms. 1996;25(1):53-61.
16. Wiklund T, Dalsgaard I. Association of *Flavobacterium psychrophilum* with rainbow trout (*Oncorhynchus mykiss*) kidney phagocytes *in vitro*. Fish & shellfish immunology. 2003;15(5):387-95. Epub 2003/10/11. PubMed PMID: 14550665.
17. Bertolini JM, Wakabayashi H, Watral VG, Whipple MJ, Rohovec JS. Electrophoretic detection of proteases from selected strains of *Flexibacter psychrophilus* and assesment of their variability. Journal of aquatic animal health. 1994;6:224-33.

18. Hogfors-Ronnholm E, Wiklund T. Hemolytic activity in *Flavobacterium psychrophilum* is a contact-dependent, two-step mechanism and differently expressed in smooth and rough phenotypes. Microbial pathogenesis. 2010;49(6):369-75. Epub 2010/09/08. doi: 10.1016/j.micpath.2010.08.002. PubMed PMID: 20817089.
19. Otis EJ. Lesions of cold-water disease in steelhead trout (*Salmo gairdneri*): the role of *Cytophaga psychrophila* extracellular products. [MSc thesis]: University of Rhode Island, Kingston; 1984.
20. Papadopoulou A, Dalsgaard I, Linden A, Wiklund T. *In vivo* adherence of *Flavobacterium psychrophilum* to mucosal external surfaces of rainbow trout (*Oncorhynchus mykiss*) fry. Journal of fish diseases. 2017;40(10):1309-20. Epub 2017/02/12. doi: 10.1111/jfd.12603. PubMed PMID: 28188658.
21. Barbier P, Rochat T, Mohammed HH, Wiens GD, Bernardet JF, Halpern D, et al. The type IX secretion system is required for virulence of the fish pathogen *Flavobacterium psychrophilum*. Applied and environmental microbiology. 2020;86(16). Epub 2020/06/14. doi: 10.1128/AEM.00799-20. PubMed PMID: 32532872.
22. Duchaud E, Boussaha M, Loux V, Bernardet JF, Michel C, Kerouault B, et al. Complete genome sequence of the fish pathogen *Flavobacterium psychrophilum*. Nature biotechnology. 2007;25(7):763-9. Epub 2007/06/27. doi: 10.1038/nbt1313. PubMed PMID: 17592475.
23. Pérez-Pascual D, Rochat T, Kerouault B, Gomez E, Neulat-Ripoll F, Henry C, et al. More than gliding: Involvement of GldD and GldG in the virulence of *Flavobacterium psychrophilum*. Frontiers in microbiology. 2017;8:2168. doi: 10.3389/fmicb.2017.02168. PubMed PMID: 29163446; PubMed Central PMCID: PMCPMC5682007.
24. Langevin C, Blanco M, Martin SA, Jouneau L, Bernardet JF, Houel A, et al. Transcriptional responses of resistant and susceptible fish clones to the bacterial pathogen *Flavobacterium psychrophilum*. PloS one. 2012;7(6):e39126. Epub 2012/06/22. doi: 10.1371/journal.pone.0039126. PubMed PMID: 22720048; PubMed Central PMCID: PMC3374740.
25. Marancik D, Gao G, Paneru B, Ma H, Hernandez AG, Salem M, et al. Whole-body transcriptome of selectively bred, resistant-, control-, and susceptible-line rainbow trout following experimental challenge with *Flavobacterium psychrophilum*. Frontiers in genetics. 2014;5:453. Epub 2015/01/27. doi: 10.3389/fgene.2014.00453. PubMed PMID: 25620978; PubMed Central PMCID: PMC4288049.
26. Skaar EP. The battle for iron between bacterial pathogens and their vertebrate hosts. PLoS pathogens. 2010;6(8):e1000949. Epub 2010/08/17. doi: 10.1371/journal.ppat.1000949. PubMed PMID: 20711357; PubMed Central PMCID: PMCPMC2920840.
27. Schauer K, Rodionov DA, de Reuse H. New substrates for TonB-dependent transport: do we only see the 'tip of the iceberg'? Trends Biochem Sci. 2008;33(7):330-8. Epub 2008/06/10. doi: 10.1016/j.tibs.2008.04.012. PubMed PMID: 18539464.
28. Andrews SC, Robinson AK, Rodriguez-Quinones F. Bacterial iron homeostasis. FEMS Microbiol Rev. 2003;27(2-3):215-37. Epub 2003/06/28. doi: 10.1016/S0168-6445(03)00055-X. PubMed PMID: 12829269.
29. Moller JD, Ellis AE, Barnes AC, Dalsgaard I. Iron acquisition mechanisms of *Flavobacterium psychrophilum*. Journal of fish diseases. 2005;28(7):391-8. Epub 2005/08/09. doi: 10.1111/j.1365-2761.2005.00639.x. PubMed PMID: 16083444.
30. Alvarez B, Alvarez J, Menendez A, Guijarro JA. A mutant in one of two *exbD* loci of a TonB system in *Flavobacterium psychrophilum* shows attenuated virulence and confers protection against cold water disease. Microbiology (Reading, England). 2008;154(Pt 4):1144-51. Epub 2008/04/01. doi: 10.1099/mic.0.2007/010900-0. PubMed PMID: 18375806.
31. Guérin C, Lee B-H, Fradet B, van Dijk E, Mirauta B, Thermes C, et al. Transcriptome architecture and regulation at environmental transitions in flavobacteria: the case of an important fish pathogen. ISME Communications. 2021;1(1):33. doi: 10.1038/s43705-021-00029-9.
32. Duchaud E, Rochat T, Habib C, Barbier P, Loux V, Guerin C, et al. Genomic diversity and evolution of the fish pathogen *Flavobacterium psychrophilum*. Frontiers in microbiology. 2018;9:138. doi: 10.3389/fmicb.2018.00138. PubMed PMID: 29467746; PubMed Central PMCID: PMCPMC5808330.
33. Krewulak KD, Vogel HJ. Structural biology of bacterial iron uptake. Biochim Biophys Acta. 2008;1778(9):1781-804. Epub 20070819. doi: 10.1016/j.bbamem.2007.07.026. PubMed PMID: 17916327.
34. Bielecki M, Antonyuk S, Strange RW, Sieminska K, Smalley JW, Mackiewicz P, et al. *Prevotella intermedia* produces two proteins homologous to *Porphyromonas gingivalis* HmuY but with different heme coordination mode. Biochem J. 2020;477(2):381-405. Epub 2020/01/04. doi: 10.1042/BCJ20190607. PubMed PMID: 31899475.
35. Bielecki M, Antonyuk S, Strange RW, Smalley JW, Mackiewicz P, Smiga M, et al. *Tannerella forsythia* Tfo belongs to *Porphyromonas gingivalis* HmuY-like family of proteins but differs in heme-binding properties.

Biosci Rep. 2018;38(5). Epub 2018/09/30. doi: 10.1042/BSR20181325. PubMed PMID: 30266745; PubMed Central PMCID: PMCPMC6200708.
36. Olczak T, Sroka A, Potempa J, Olczak M. *Porphyromonas gingivalis* HmuY and HmuR: further characterization of a novel mechanism of heme utilization. Arch Microbiol. 2008;189(3):197-210. Epub 2007/10/09. doi: 10.1007/s00203-007-0309-7. PubMed PMID: 17922109; PubMed Central PMCID: PMCPMC2577367.
37. Sieminska K, Cierpisz P, Smiga M, Olczak T. *Porphyromonas gingivalis* HmuY and *Bacteroides vulgatus* Bvu-A Novel Competitive Heme Acquisition Strategy. Int J Mol Sci. 2021;22(5). Epub 2021/03/07. doi: 10.3390/ijms22052237. PubMed PMID: 33668119; PubMed Central PMCID: PMCPMC7956564.
38. Baez WD, Roy B, McNutt ZA, Shatoff EA, Chen S, Bundschuh R, et al. Global analysis of protein synthesis in *Flavobacterium johnsoniae* reveals the use of Kozak-like sequences in diverse bacteria. Nucleic acids research. 2019;47(20):10477-88. Epub 2019/10/12. doi: 10.1093/nar/gkz855. PubMed PMID: 31602466; PubMed Central PMCID: PMCPMC6847099.
39. Meheust R, Huang S, Rivera-Lugo R, Banfield JF, Light SH. Post-translational flavinylation is associated with diverse extracytosolic redox functionalities throughout bacterial life. Elife. 2021;10. Epub 20210525. doi: 10.7554/eLife.66878. PubMed PMID: 34032212; PubMed Central PMCID: PMCPMC8238504.
40. Chandrangsu P, Rensing C, Helmann JD. Metal homeostasis and resistance in bacteria. Nature reviews Microbiology. 2017;15(6):338-50. Epub 2017/03/28. doi: 10.1038/nrmicro.2017.15. PubMed PMID: 28344348; PubMed Central PMCID: PMCPMC5963929.
41. Troxell B, Hassan HM. Transcriptional regulation by Ferric Uptake Regulator (Fur) in pathogenic bacteria. Front Cell Infect Microbiol. 2013;3:59. Epub 2013/10/10. doi: 10.3389/fcimb.2013.00059. PubMed PMID: 24106689; PubMed Central PMCID: PMCPMC3788343.
42. Dent AT, Mourino S, Huang W, Wilks A. Post-transcriptional regulation of the *Pseudomonas aeruginosa* heme assimilation system (Has) fine-tunes extracellular heme sensing. The Journal of biological chemistry. 2019;294(8):2771-85. Epub 2018/12/30. doi: 10.1074/jbc.RA118.006185. PubMed PMID: 30593511; PubMed Central PMCID: PMCPMC6393591.
43. Rochat T, Bouloc P, Repoila F. Gene expression control by selective RNA processing and stabilization in bacteria. FEMS microbiology letters. 2013;344(2):104-13. Epub 2013/04/27. doi: 10.1111/1574-6968.12162. PubMed PMID: 23617839.
44. Obana N, Shirahama Y, Abe K, Nakamura K. Stabilization of *Clostridium perfringens* collagenase mRNA by VR-RNA-dependent cleavage in 5' leader sequence. Mol Microbiol. 2010;77(6):1416-28. Epub 2010/06/25. doi: 10.1111/j.1365-2958.2010.07258.x. PubMed PMID: 20572941.
45. Levipan HA, Avendano-Herrera R. Different phenotypes of mature biofilm in *Flavobacterium psychrophilum* share a potential for virulence that differs from planktonic state. Front Cell Infect Microbiol. 2017;7:76. Epub 2017/04/01. doi: 10.3389/fcimb.2017.00076. PubMed PMID: 28361040; PubMed Central PMCID: PMCPMC5350093.
46. Morro B, Doherty MK, Balseiro P, Handeland SO, MacKenzie S, Sveier H, et al. Plasma proteome profiling of freshwater and seawater life stages of rainbow trout (*Oncorhynchus mykiss*). PloS one. 2020;15(1):e0227003. Epub 2020/01/04. doi: 10.1371/journal.pone.0227003. PubMed PMID: 31899766; PubMed Central PMCID: PMCPMC6941806.
47. Ascenzi P, di Masi A, Leboffe L, Frangipani E, Nardini M, Verde C, et al. Structural Biology of Bacterial Haemophores. Adv Microb Physiol. 2015;67:127-76. Epub 2015/12/01. doi: 10.1016/bs.ampbs.2015.09.002. PubMed PMID: 26616517.
48. Izadi-Pruneyre N, Huche F, Lukat-Rodgers GS, Lecroisey A, Gilli R, Rodgers KR, et al. The heme transfer from the soluble HasA hemophore to its membrane-bound receptor HasR is driven by protein-protein interaction from a high to a lower affinity binding site. The Journal of biological chemistry. 2006;281(35):25541-50. Epub 2006/06/16. doi: 10.1074/jbc.M603698200. PubMed PMID: 16774915.
49. Press CM, Evensen Ø. The morphology of the immune system in teleost fishes. Fish & shellfish immunology. 1999;9(4):309-18. doi: https://doi.org/10.1006/fsim.1998.0181.
50. Martinez FJ, Garcia-Riera MP, Ganteras M, De Costa J, Zamora S. Blood parameters in rainbow trout (*Oncorhynchus mykiss*): Simultaneous influence of various factors. Comparative Biochemistry and Physiology Part A: Physiology. 1994;107(1):95-100. doi: https://doi.org/10.1016/0300-9629(94)90279-8.
51. Anzaldi LL, Skaar EP. Overcoming the heme paradox: heme toxicity and tolerance in bacterial pathogens. Infection and immunity. 2010;78(12):4977-89. Epub 2010/08/04. doi: 10.1128/IAI.00613-10. PubMed PMID: 20679437; PubMed Central PMCID: PMCPMC2981329.

52. Otero-Asman JR, Garcia-Garcia AI, Civantos C, Quesada JM, Llamas MA. *Pseudomonas aeruginosa* possesses three distinct systems for sensing and using the host molecule haem. Environ Microbiol. 2019;21(12):4629-47. Epub 20190908. doi: 10.1111/1462-2920.14773. PubMed PMID: 31390127.
53. Smith AD, Wilks A. Differential contributions of the outer membrane receptors PhuR and HasR to heme acquisition in *Pseudomonas aeruginosa*. The Journal of biological chemistry. 2015;290(12):7756-66. Epub 2015/01/27. doi: 10.1074/jbc.M114.633495. PubMed PMID: 25616666; PubMed Central PMCID: PMCPMC4367277.
54. Bracken CS, Baer MT, Abdur-Rashid A, Helms W, Stojiljkovic I. Use of heme-protein complexes by the *Yersinia enterocolitica* HemR receptor: histidine residues are essential for receptor function. Journal of bacteriology. 1999;181(19):6063-72. Epub 1999/09/28. doi: 10.1128/JB.181.19.6063-6072.1999. PubMed PMID: 10498719; PubMed Central PMCID: PMCPMC103634.
55. Fusco WG, Choudhary NR, Council SE, Collins EJ, Leduc I. Mutational analysis of hemoglobin binding and heme utilization by a bacterial hemoglobin receptor. Journal of bacteriology. 2013;195(13):3115-23. Epub 2013/05/15. doi: 10.1128/JB.00199-13. PubMed PMID: 23667232; PubMed Central PMCID: PMCPMC3697543.
56. Liu X, Olczak T, Guo HC, Dixon DW, Genco CA. Identification of amino acid residues involved in heme binding and hemoprotein utilization in the *Porphyromonas gingivalis* heme receptor HmuR. Infection and immunity. 2006;74(2):1222-32. Epub 2006/01/24. doi: 10.1128/IAI.74.2.1222-1232.2006. PubMed PMID: 16428772; PubMed Central PMCID: PMCPMC1360300.
57. Gray DA, White JBR, Oluwole AO, Rath P, Glenwright AJ, Mazur A, et al. Insights into SusCD-mediated glycan import by a prominent gut symbiont. Nature communications. 2021;12(1):44. Epub 2021/01/06. doi: 10.1038/s41467-020-20285-y. PubMed PMID: 33398001; PubMed Central PMCID: PMCPMC7782687.
58. Wojtowicz H, Guevara T, Tallant C, Olczak M, Sroka A, Potempa J, et al. Unique structure and stability of HmuY, a novel heme-binding protein of *Porphyromonas gingivalis*. PLoS pathogens. 2009;5(5):e1000419. Epub 2009/05/09. doi: 10.1371/journal.ppat.1000419. PubMed PMID: 19424422; PubMed Central PMCID: PMCPMC2671838.
59. Castillo D, Jorgensen J, Sundell K, Madsen L, Dalsgaard I, Wiklund T, et al. Genome-informed approach to identify genetic determinants of *Flavobacterium psychrophilum* phage susceptibility. Environ Microbiol. 2021. Epub 2021/05/15. doi: 10.1111/1462-2920.15593. PubMed PMID: 33989443.
60. Cisar JO, Bush CA, Wiens GD. Comparative Structural and Antigenic Characterization of Genetically Distinct *Flavobacterium psychrophilum* O-Polysaccharides. Frontiers in microbiology. 2019;10:1041. Epub 2019/05/30. doi: 10.3389/fmicb.2019.01041. PubMed PMID: 31139169; PubMed Central PMCID: PMCPMC6519341.
61. Madsen L, Dalsgaard I. Comparative studies of Danish *Flavobacterium psychrophilum* isolates: ribotypes, plasmid profiles, serotypes and virulence. 2000.
62. Ngo TP, Bartie KL, Thompson KD, Verner-Jeffreys DW, Hoare R, Adams A. Genetic and serological diversity of *Flavobacterium psychrophilum* isolates from salmonids in United Kingdom. Veterinary microbiology. 2017;201:216-24. doi: 10.1016/j.vetmic.2017.01.032. PubMed PMID: 28284613.
63. Rochat T, Fujiwara-Nagata E, Calvez S, Dalsgaard I, Madsen L, Calteau A, et al. Genomic Characterization of *Flavobacterium psychrophilum* Serotypes and Development of a Multiplex PCR-Based Serotyping Scheme. Frontiers in microbiology. 2017;8:1752. doi: 10.3389/fmicb.2017.01752. PubMed PMID: 28955320; PubMed Central PMCID: PMCPMC5601056.
64. Rochat T, Pérez-Pascual D, Nilsen H, Carpentier M, Bridel S, Bernardet JF, et al. Identification of a novel elastin-degrading enzyme from the fish pathogen *Flavobacterium psychrophilum*. Applied and environmental microbiology. 2019. Epub 2019/01/13. doi: 10.1128/AEM.02535-18. PubMed PMID: 30635380.
65. Sundell K, Landor L, Nicolas P, Jorgensen J, Castillo D, Middelboe M, et al. Phenotypic and Genetic Predictors of Pathogenicity and Virulence in *Flavobacterium psychrophilum*. Frontiers in microbiology. 2019;10:1711. Epub 2019/08/10. doi: 10.3389/fmicb.2019.01711. PubMed PMID: 31396199; PubMed Central PMCID: PMCPMC6668605.
66. Shisaka Y, Iwai Y, Yamada S, Uehara H, Tosha T, Sugimoto H, et al. Hijacking the heme acquisition system of *Pseudomonas aeruginosa* for the delivery of phthalocyanine as an antimicrobial. ACS Chem Biol. 2019;14(7):1637-42. Epub 20190709. doi: 10.1021/acschembio.9b00373. PubMed PMID: 31287285.
67. Rochat T, Barbier P, Nicolas P, Loux V, Perez-Pascual D, Guijarro JA, et al. Complete genome sequence of *Flavobacterium psychrophilum* strain OSU THCO2-90, used for functional genetic analysis. Genome announcements. 2017;5(8). doi: 10.1128/genomeA.01665-16. PubMed PMID: 28232446; PubMed Central PMCID: PMCPMC5323625.

68. Vallenet D, Calteau A, Cruveiller S, Gachet M, Lajus A, Josso A, et al. MicroScope in 2017: an expanding and evolving integrated resource for community expertise of microbial genomes. Nucleic acids research. 2017;45(D1):D517-D28. doi: 10.1093/nar/gkw1101. PubMed PMID: 27899624; PubMed Central PMCID: PMCPMC5210572.
69. Pei J, Kim BH, Grishin NV. PROMALS3D: a tool for multiple protein sequence and structure alignments. Nucleic acids research. 2008;36(7):2295-300. Epub 2008/02/22. doi: 10.1093/nar/gkn072. PubMed PMID: 18287115; PubMed Central PMCID: PMCPMC2367709.
70. Zhu Y, Thomas F, Larocque R, Li N, Duffieux D, Cladiere L, et al. Genetic analyses unravel the crucial role of a horizontally acquired alginate lyase for brown algal biomass degradation by *Zobellia galactanivorans*. Environ Microbiol. 2017;19(6):2164-81. Epub 2017/02/17. doi: 10.1111/1462-2920.13699. PubMed PMID: 28205313.
71. Alvarez B, Secades P, McBride MJ, Guijarro JA. Development of genetic techniques for the psychrotrophic fish pathogen *Flavobacterium psychrophilum*. Applied and environmental microbiology. 2004;70(1):581-7. Epub 2004/01/09. doi: 10.1128/AEM.70.1.581-587.2004. PubMed PMID: 14711690; PubMed Central PMCID: PMCPMC321288.
72. Lechardeur D, Cesselin B, Liebl U, Vos MH, Fernandez A, Brun C, et al. Discovery of intracellular heme-binding protein HrtR, which controls heme efflux by the conserved HrtB-HrtA transporter in *Lactococcus lactis*. The Journal of biological chemistry. 2012;287(7):4752-8. Epub 2011/11/16. doi: 10.1074/jbc.M111.297531. PubMed PMID: 22084241; PubMed Central PMCID: PMCPMC3281666.
73. Mandl CW, Heinz FX, Puchhammer-Stockl E, Kunz C. Sequencing the termini of capped viral RNA by 5'-3' ligation and PCR. Biotechniques. 1991;10(4):484, 6. Epub 1991/04/01. PubMed PMID: 1651093.
74. Quillet E, Dorson M, Le Guillou S, Benmansour A, Boudinot P. Wide range of susceptibility to rhabdoviruses in homozygous clones of rainbow trout. Fish & shellfish immunology. 2007;22(5):510-9.

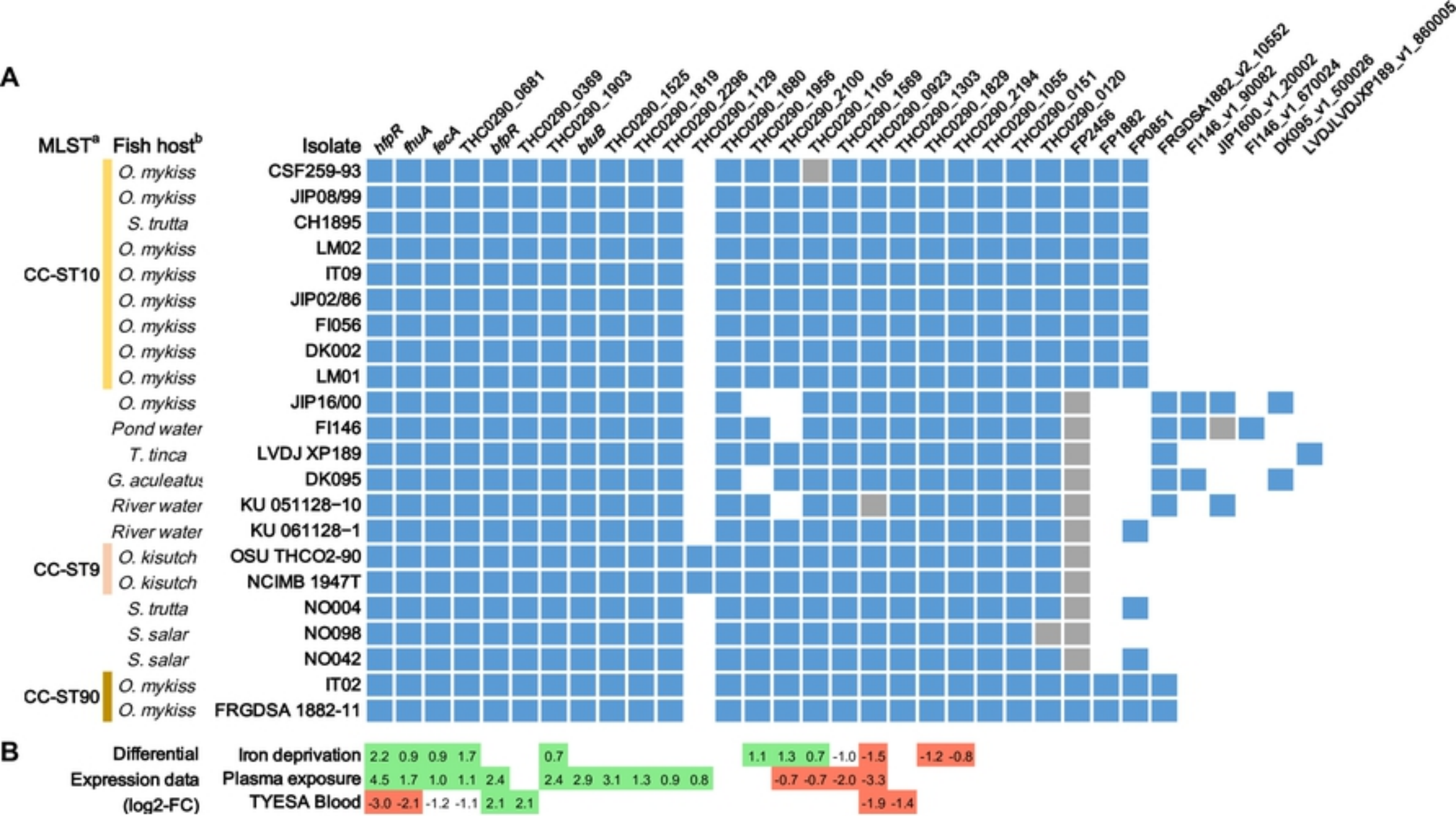
A
MLST[a]
Fish host[b]
Isolate
hfpR
fhuA
fecA
THC0290_0681
bfpR
THC0290_0369
THC0290_1903
btuB
THC0290_1525
THC0290_1819
THC0290_2296
THC0290_1129
THC0290_1680
THC0290_1956
THC0290_2100
THC0290_1105
THC0290_1569
THC0290_0923
THC0290_1303
THC0290_1829
THC0290_2194
THC0290_1055
THC0290_0151
THC0290_0120
FP2456
FP1882
FP0851
FRGDSA1882_v2_10552
FI146_v1_90082
JIP1600_v1_20002
FI146_v1_670024
DK095_v1_500026
LVDJLVDJXP189_v1_860005
CC-ST10
O. mykiss CSF259-93
O. mykiss JIP08/99
S. trutta CH1895
O. mykiss LM02
O. mykiss IT09
O. mykiss JIP02/86
O. mykiss FI056
O. mykiss DK002
O. mykiss LM01
O. mykiss JIP16/00
Pond water FI146
T. tinca LVDJ XP189
G. aculeatus DK095
River water KU 051128−10
River water KU 061128−1
CC-ST9
O. kisutch OSU THCO2-90
O. kisutch NCIMB 1947T
S. trutta NO004
S. salar NO098
S. salar NO042
CC-ST90
O. mykiss IT02
O. mykiss FRGDSA 1882-11
B
Differential Expression data (log2-FC)
Iron deprivation 2.2 0.9 0.9 1.7 0.7 1.1 1.3 0.7 -1.0 -1.5 -1.2 -0.8
Plasma exposure 4.5 1.7 1.0 1.1 2.4 2.4 2.9 3.1 1.3 0.9 0.8 -0.7 -0.7 -2.0 -3.3
TYESA Blood -3.0 -2.1 -1.2 -1.1 2.1 2.1 -1.9 -1.4

Fig1

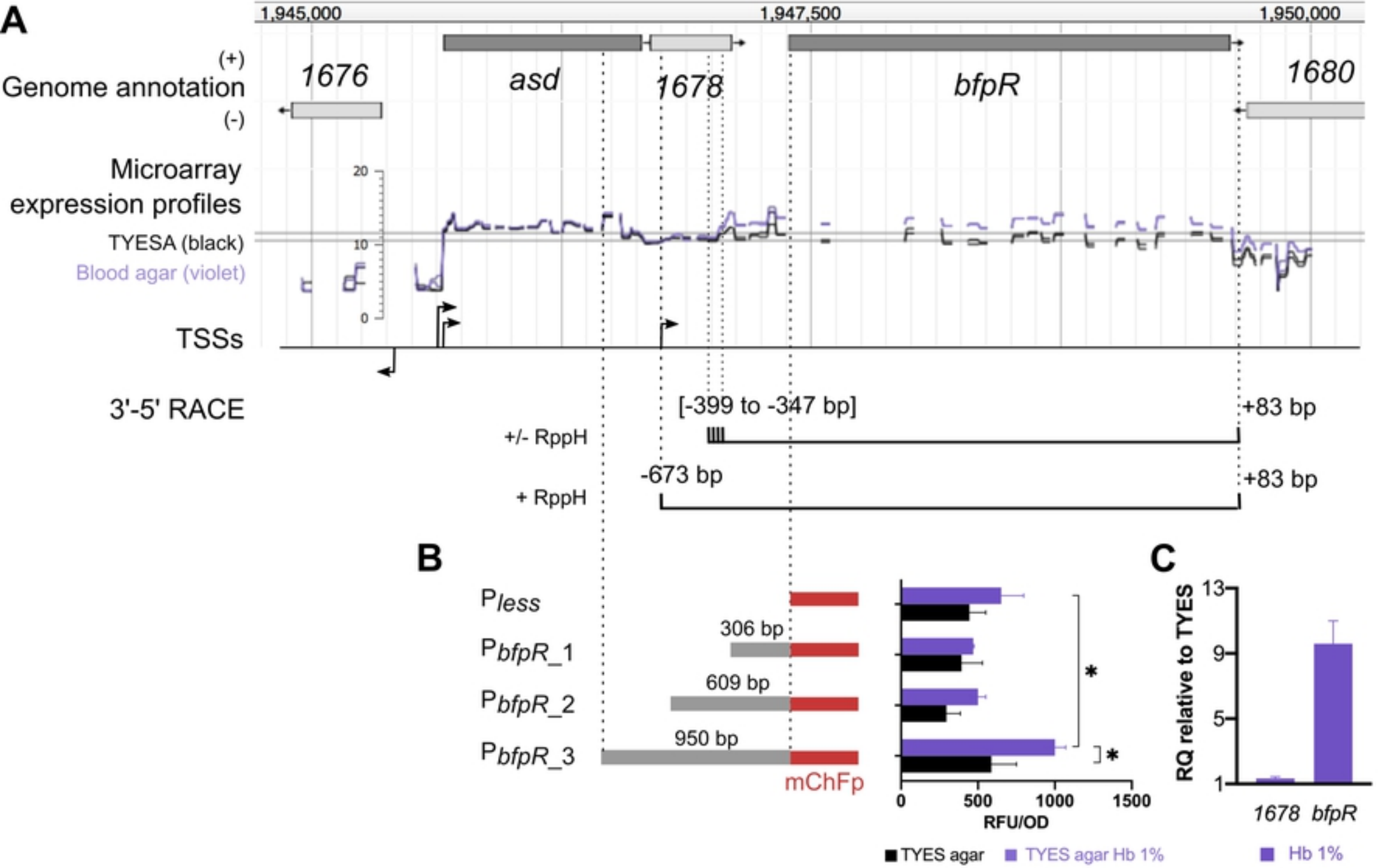
A
1,945,000
1,947,500
1,950,000
(+)
Genome annotation
(-)
1676
asd
1678
bfpR
1680
Microarray
expression profiles
TYESA (black)
Blood agar (violet)
20
10
0
TSSs
3'-5' RACE
[-399 to -347 bp]
+83 bp
+/- RppH
-673 bp
+83 bp
+ RppH
B
Pless
306 bp
PbfpR_1
609 bp
PbfpR_2
950 bp
PbfpR_3
mChFp
0
500
1000
1500
RFU/OD
*
*
TYES agar
TYES agar Hb 1%
C
RQ relative to TYES
13
9
5
1
1678
bfpR
Hb 1%

Fig2

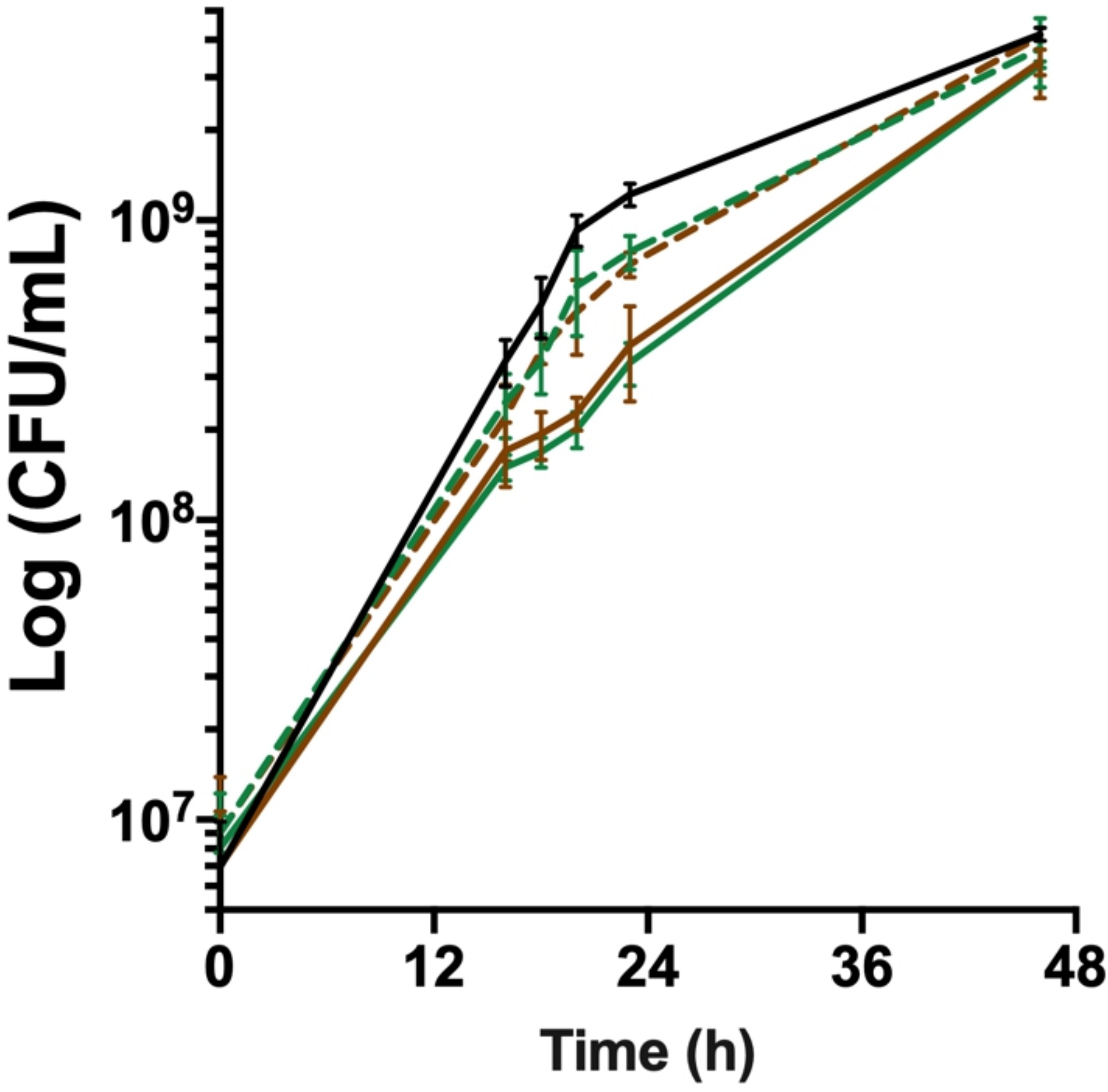


Fig3

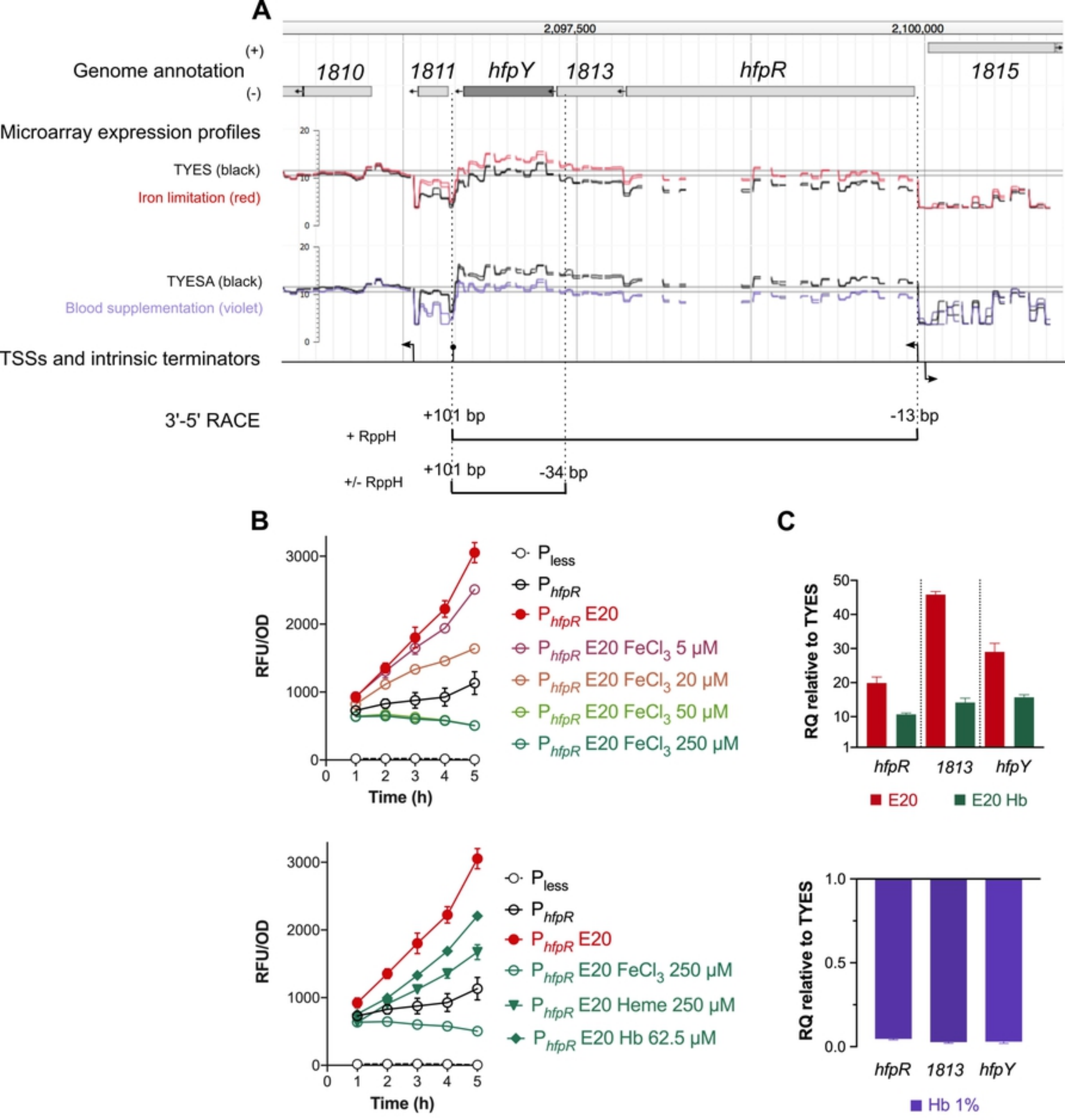
A
2,097,500
2,100,000
Genome annotation
(+)
(-)
1810
1811
hfpY
1813
hfpR
1815
Microarray expression profiles
TYES (black)
Iron limitation (red)
TYESA (black)
Blood supplementation (violet)
TSSs and intrinsic terminators
3'-5' RACE
+ RppH
+101 bp
-13 bp
+/- RppH
+101 bp
-34 bp
B
RFU/OD
Time (h)
P less
P hfpR
P hfpR E20
P hfpR E20 FeCl3 5 µM
P hfpR E20 FeCl3 20 µM
P hfpR E20 FeCl3 50 µM
P hfpR E20 FeCl3 250 µM
P hfpR E20 Heme 250 µM
P hfpR E20 Hb 62.5 µM
C
RQ relative to TYES
hfpR
1813
hfpY
E20
E20 Hb
Hb 1%

Fig4

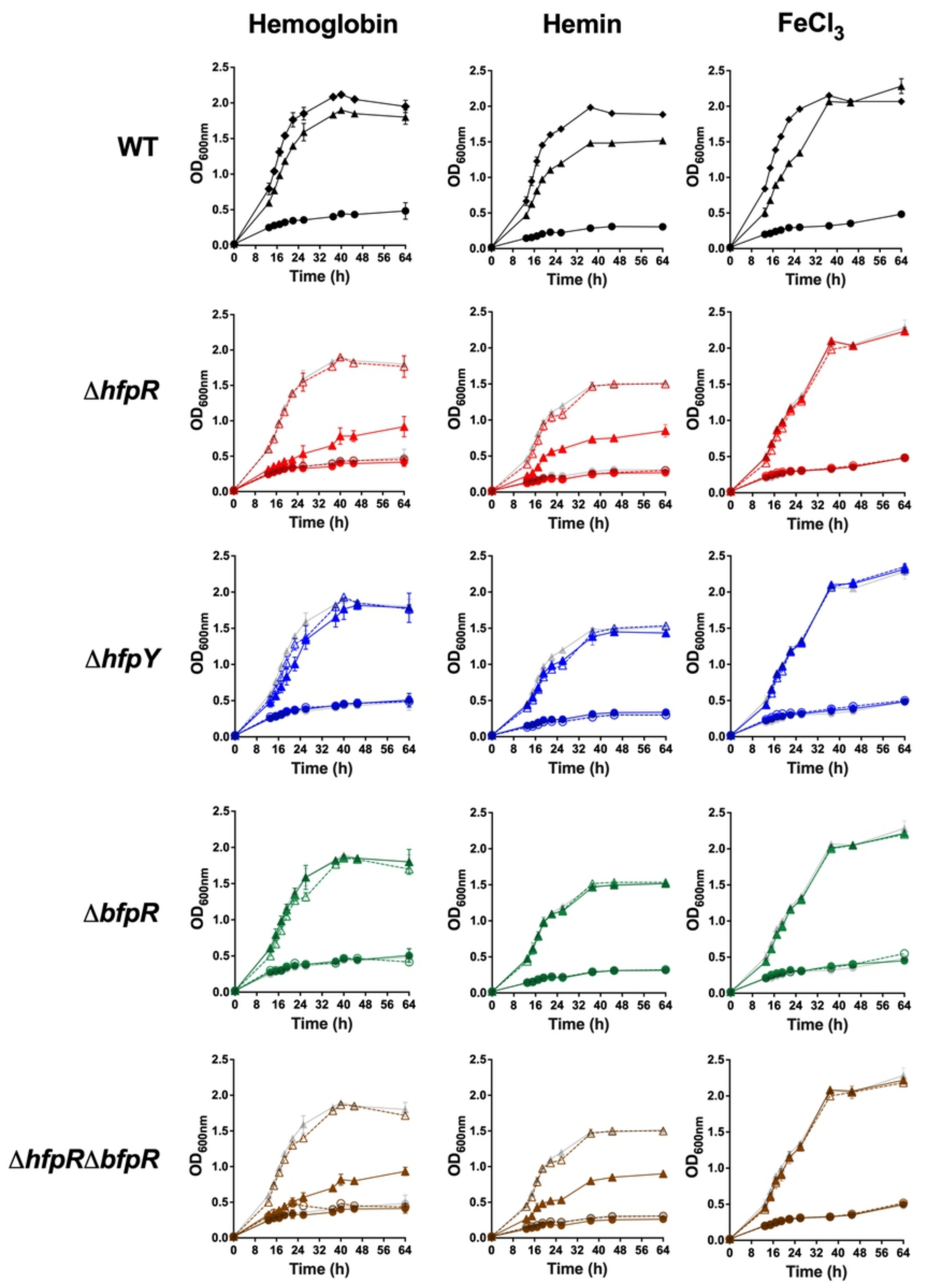
Hemoglobin
Hemin
FeCl3
WT
ΔhfpR
ΔhfpY
ΔbfpR
ΔhfpRΔbfpR
OD600nm
Time (h)
0.0
0.5
1.0
1.5
2.0
2.5
0
8
16
24
32
40
48
56
64

Fig5

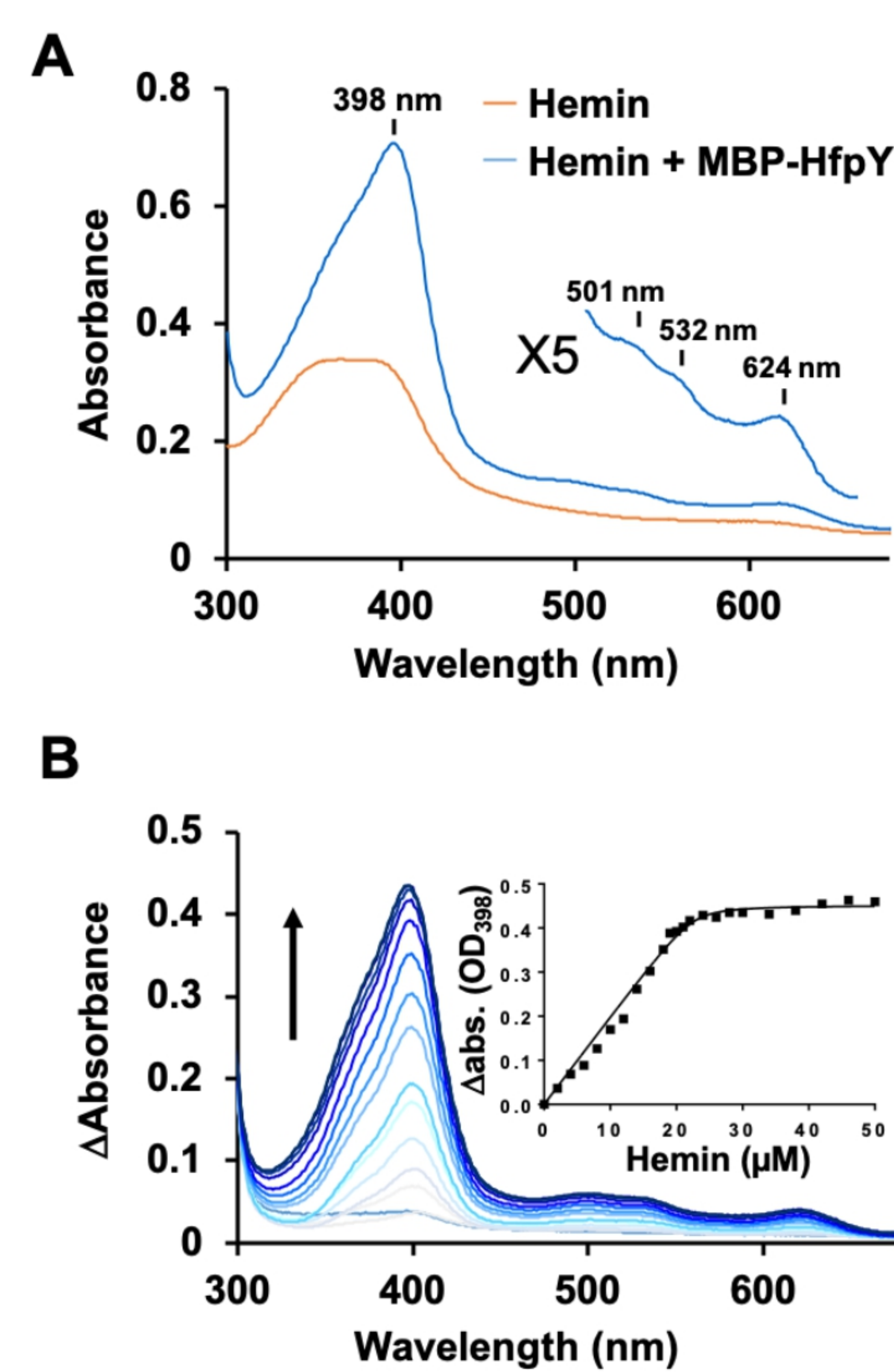
A
0.8
0.6
0.4
0.2
0
Absorbance
398 nm
Hemin
Hemin + MBP-HfpY
501 nm
532 nm
624 nm
X5
300
400
500
600
Wavelength (nm)
B
0.5
0.4
0.3
0.2
0.1
0
ΔAbsorbance
300
400
500
600
Wavelength (nm)
Δabs. (OD398)
0.5
0.4
0.3
0.2
0.1
0.0
0
10
20
30
40
50
Hemin (μM)

Fig6

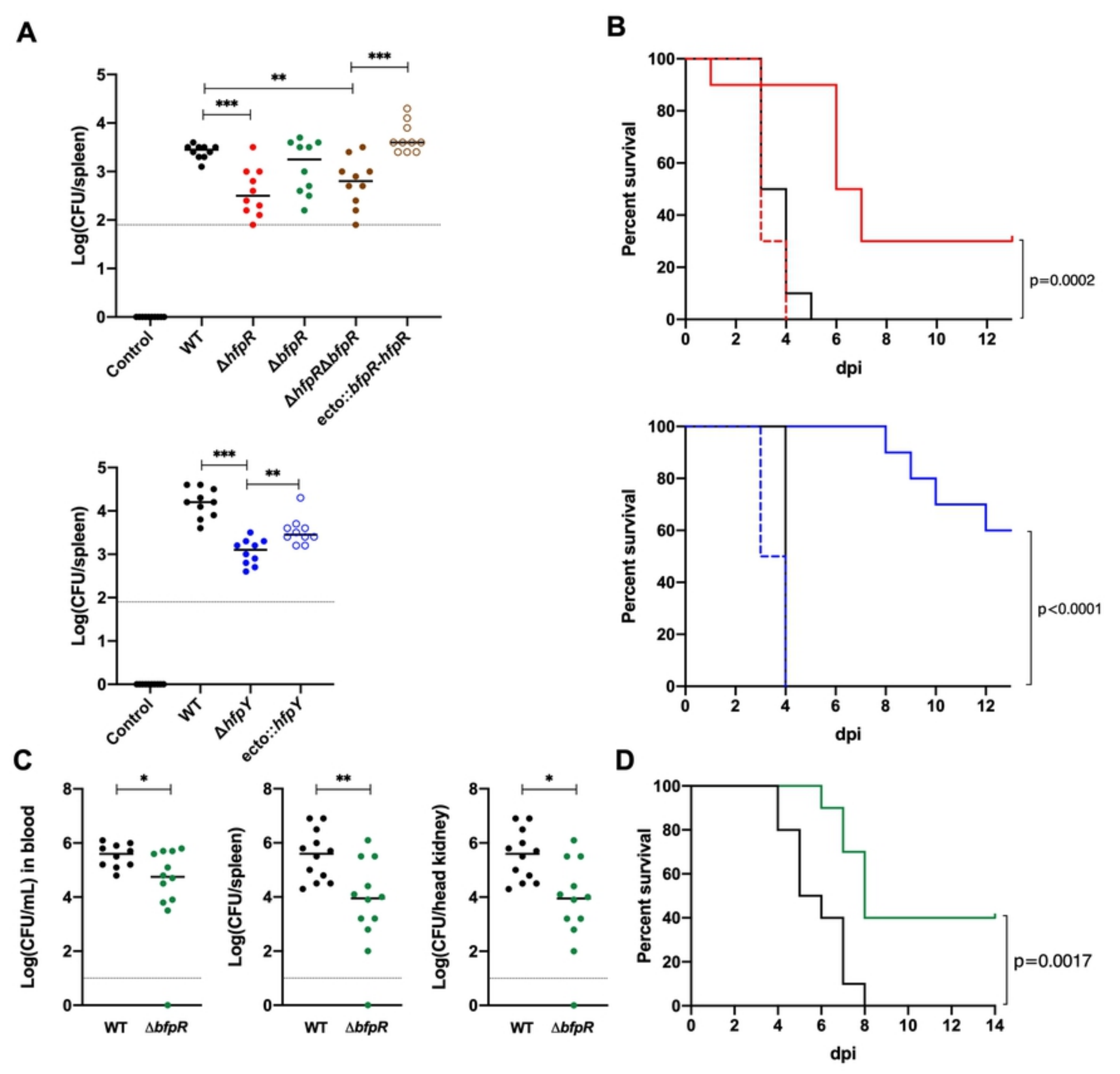
A
Log(CFU/spleen)
Control
WT
ΔhfpR
ΔbfpR
ΔhfpRΔbfpR
ecto::bfpR-hfpR
Log(CFU/spleen)
Control
WT
ΔhfpY
ecto::hfpY
B
Percent survival
dpi
p=0.0002
Percent survival
dpi
p<0.0001
C
Log(CFU/mL) in blood
Log(CFU/spleen)
Log(CFU/head kidney)
WT
ΔbfpR
D
Percent survival
dpi
p=0.0017

Fig7

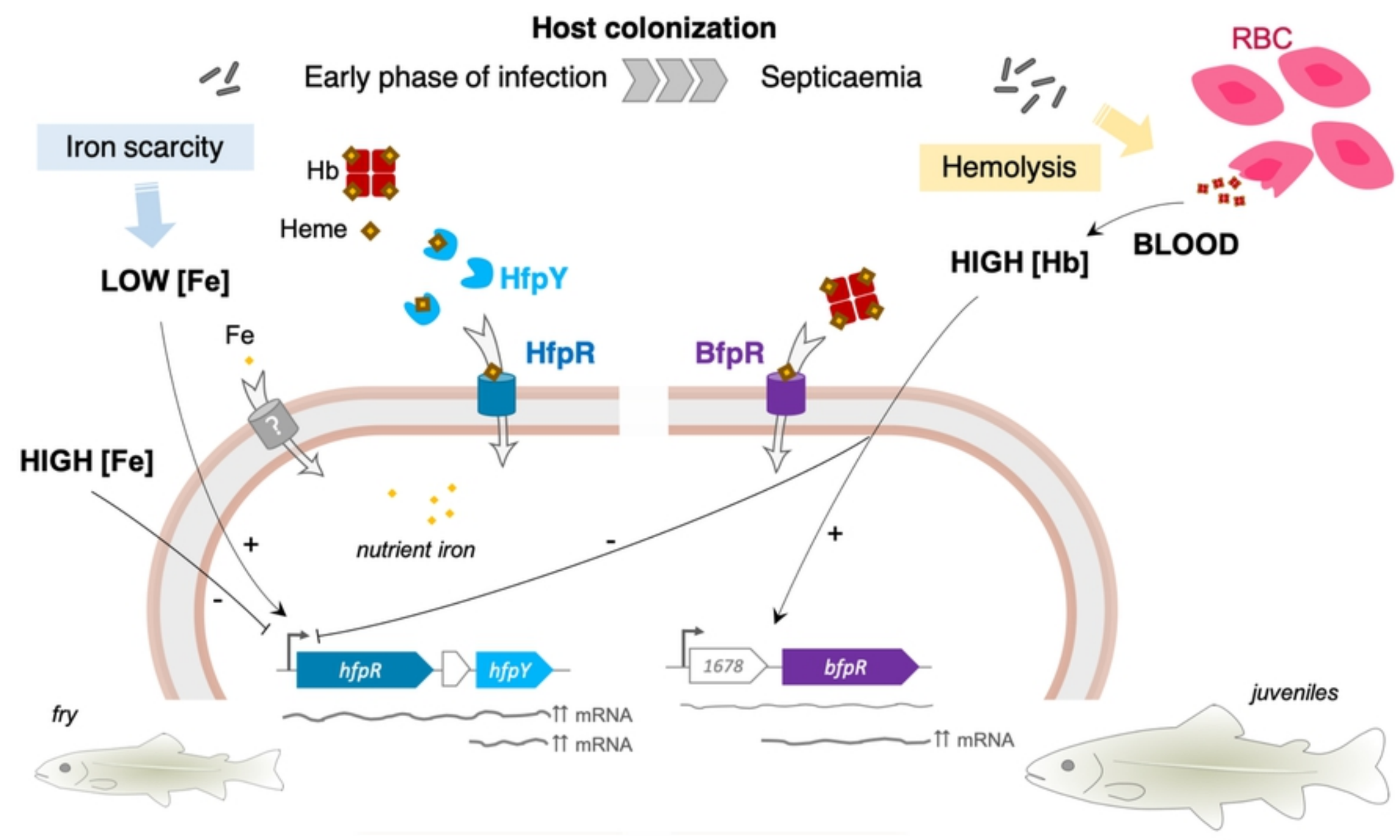
Host colonization
Early phase of infection
Septicaemia
RBC
Iron scarcity
Hb
Heme
Hemolysis
BLOOD
HIGH [Hb]
LOW [Fe]
HfpY
Fe
HfpR
BfpR
?
HIGH [Fe]
+
-
nutrient iron
-
+
hfpR
hfpY
1678
bfpR
↑↑ mRNA
↑↑ mRNA
↑↑ mRNA
fry
juveniles

Fig8